ACS OMEGA

Open Access

http://pubs.acs.org/journal/acsodf

Article

Olaparib Process Development Employing Quality by Design (QbD) Principles

Amarendhar Manda, Shravan Kumar Komati, Sekhar Munaswamy Nariyam, Sasikala Cheemalapati Venkata Annapurna, Gopal Chandru Senadi, Arthanareeswari Maruthapillai,* and Rakeshwar Bandichhor*

Cite This: *ACS Omega* 2024, 9, 30327−30349

Read Online

ACCESS | Metrics & More | Article Recommendations | Supporting Information

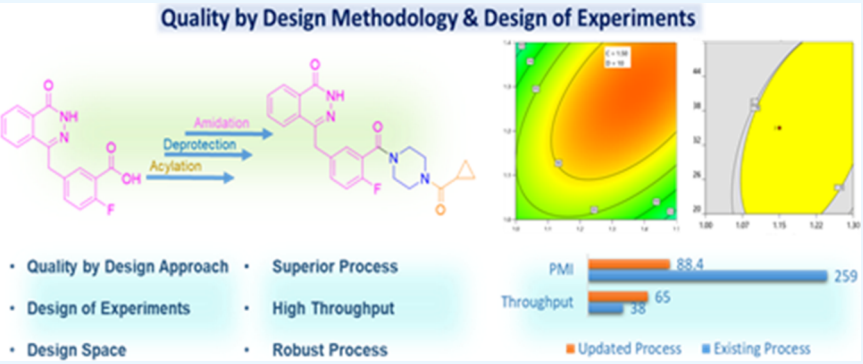

ABSTRACT: This study focuses on multivariate experimental design and statistical analysis to optimize the process of Olaparib **1**. Quality by design (QbD) methodology was adopted for optimization of the Olaparib process consisting of three reaction steps: (1) amidation, (2) deprotection, and (3) acylation. Every chemical conversion was studied in isolation, employing risk assessment to identify key material attributes and key process parameters that may have the potential to impact the reaction. Thereafter, the screening design of experiment (DoE) was employed to scrutinize the factors that significantly impacted yield. Moving forward, the scrutinized factors which were found to impact the responses, the set of critical material attributes (CMAs) and critical process parameters (CPPs), were considered for optimization by applying I-Optimal design to define design space arriving at a robust setting wherein the predefined targets were supposedly optimal. To our delight, we got 95, 91, and 75% yield with more than 99% purity in amidation, deprotection, and acetylation, respectively, which enabled us to systematically identify design space to meet the desired quality target of the product consistently. More importantly, to distinguish the CMAs and CPPs, these elements ought to be monitored to have control of the quality parameter throughout the active pharmaceutical ingredient (API) value chain until commercial manufacturing followed by marketing. Eventually, we have developed a greener process in comparison to precedented one for Olaparib **1**.

INTRODUCTION

Safety and efficacy have been efficiently built into the pharmaceutical product development process and have been integral over the years. In September 2004, the US Food and Drug Administration published its final report on "Pharmaceutical cGMP for the 21st Century—A Risk-Based Approach: Final Report,"[1] leading to the initiation of Quality by Design (QbD) coupled with process analytical technology (PAT) as tools to foresee the quality parameters starting from ideation to the product manufacturing. The traditional approach of manufacturing and testing the products against regulatory specifications

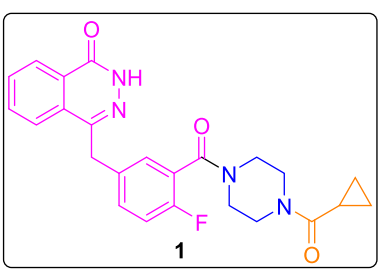

Figure 1. Chemical structure of Olaparib **1**.

Received: February 9, 2024
Revised: June 14, 2024
Accepted: June 18, 2024
Published: July 1, 2024

Scheme 1. Synthesis of Olaparib 1 at Scale

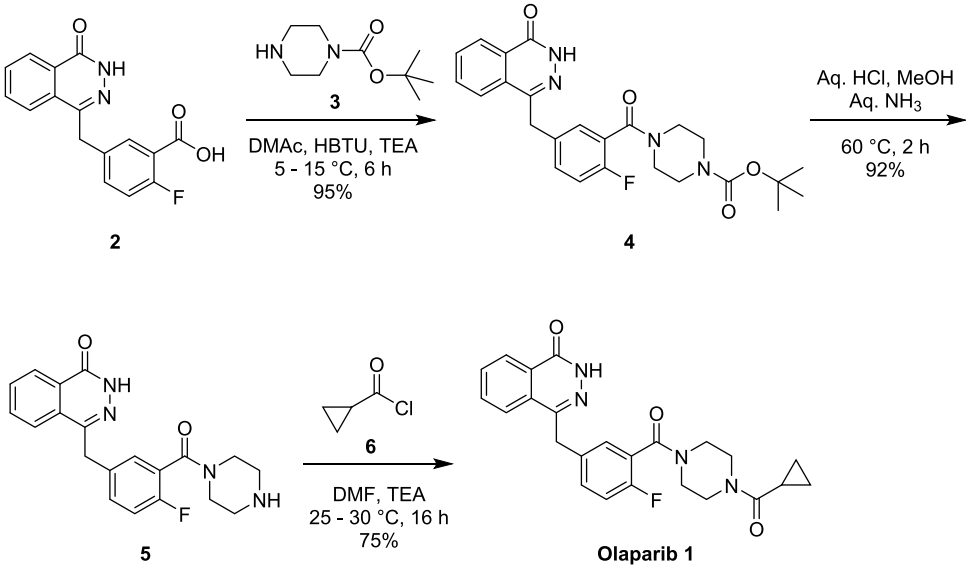

Scheme 2. Synthesis of Amide Intermediate 4

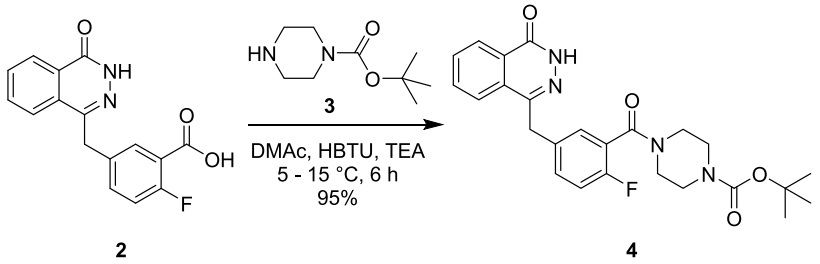

Table 1. Parameters Considered for Screening the DoE

factor	parameter	units	type	−1/L1	+1/L2
A	solvent quantity	vol	numeric	3.0	12.0
B	base	equiv	numeric	1.0	3.0
C	reagent	equiv	numeric	1.0	2.0
D	boc piperazine	equiv	numeric	1.0	2.0
E	temperature	°C	numeric	10.0	40.0
F	dilution of BP in solvent	vol	numeric	3.0	6.0
G	solvent type		categoric	DMAc	NMP
H	base type		categoric	DIPEA	TEA
J	reagent type		categoric	HBTU	EDC·HCl/HOBt·H_2O

was deemed unpredictable, poorly scientific, and substandard leading to additional costs, reworks, and regulatory consequences, e.g., market recalls due to suboptimal quality as one of the reasons.

Quality by Design was also introduced through the International Council for Harmonization of Technical Requirements for Pharmaceuticals for Human Use (ICH) guidelines[2−4] Q8, Q9, and Q10 from November 2005 to August 2009. QbD is defined as "a systematic approach to pharmaceutical development that begins with predefined objectives and emphasizes product and process understanding and process control, based on sound science and quality risk management." The guidelines laid the framework for the industry of what was expected of the regulatory bodies. Considering this fact, the desired product profile was captured as a quality target product profile (QTPP), the attributes that defined the quality of the product as critical quality attributes (CQAs). Not only the product but also the process involved should be designed in such a way that the quality, through mechanistic understanding and in-depth study of how the CPPs and CMAs would affect the CQAs, are met. Quality should not be tested into products; it must be built in by design. QbD involves identifying QTPPs, determining CQAs, linking material attributes and process parameters to CQAs, performin risk assessment, developing a design space, and implementing a control strategy and continuous improvement.[2]

The International Council for Harmonization (ICH) Q9 defines the risk assessment and the approaches that can be used for design irrespective of what stage the product is and should be integrated with ICH Q8 with ICH Q10. Risk assessment through the Ishikawa diagram, heat maps, and FMEA remain widely used tools to assess risk in the pharmaceutical industry.[7−10,20] Several precedented literature examples illustrate this approach to identify the key material attributes (KMAs) and key process parameters (KPPs) for the reaction

https://doi.org/10.1021/acsomega.4c01293
ACS Omega 2024, 9, 30327−30349

Table 2. Design Layout Along with Responses

run	A	B	C	D	E	F	G	H	J	**2** (%)	yield[a] (%)
1	1	1	1	−1	1	−1	L2	L1	L1	0.20	60.9
2	1	−1	−1	1	−1	1	L1	L1	L1	0.16	88.1
3	1	−1	−1	1	−1	1	L1	L1	L1	0.21	86.5
4	−1	1	−1	−1	−1	1	L2	L2	L1	0.12	79.6
5	1	−1	1	−1	−1	−1	L2	L2	L2	0.18	90.3
6	1	1	−1	1	1	1	L2	L2	L2	52.01	14.0
7	−1	1	1	1	−1	−1	L1	L2	L1	0.43	94.6
8	1	1	−1	1	1	1	L2	L2	L2	52.09	15.5
9	1	1	1	−1	−1	1	L1	L1	L2	4.32	62.4
10	−1	1	−1	−1	−1	1	L2	L2	L1	0.14	77.7
11	−1	−1	1	1	1	1	L2	L1	L1	0.06	85.3
12	−1	1	−1	−1	1	−1	L1	L1	L2	63.65	11.6
13	1	−1	−1	−1	1	−1	L1	L2	L1	0.53	84.8
14	−1	−1	1	−1	1	1	L1	L2	L2	1.11	62.7
15	−1	−1	−1	1	−1	−1	L2	L1	L2	18.8	55.8
16	−1	1	1	1	−1	−1	L1	L2	L1	0.06	92.0

[a]Yield after purity correction.

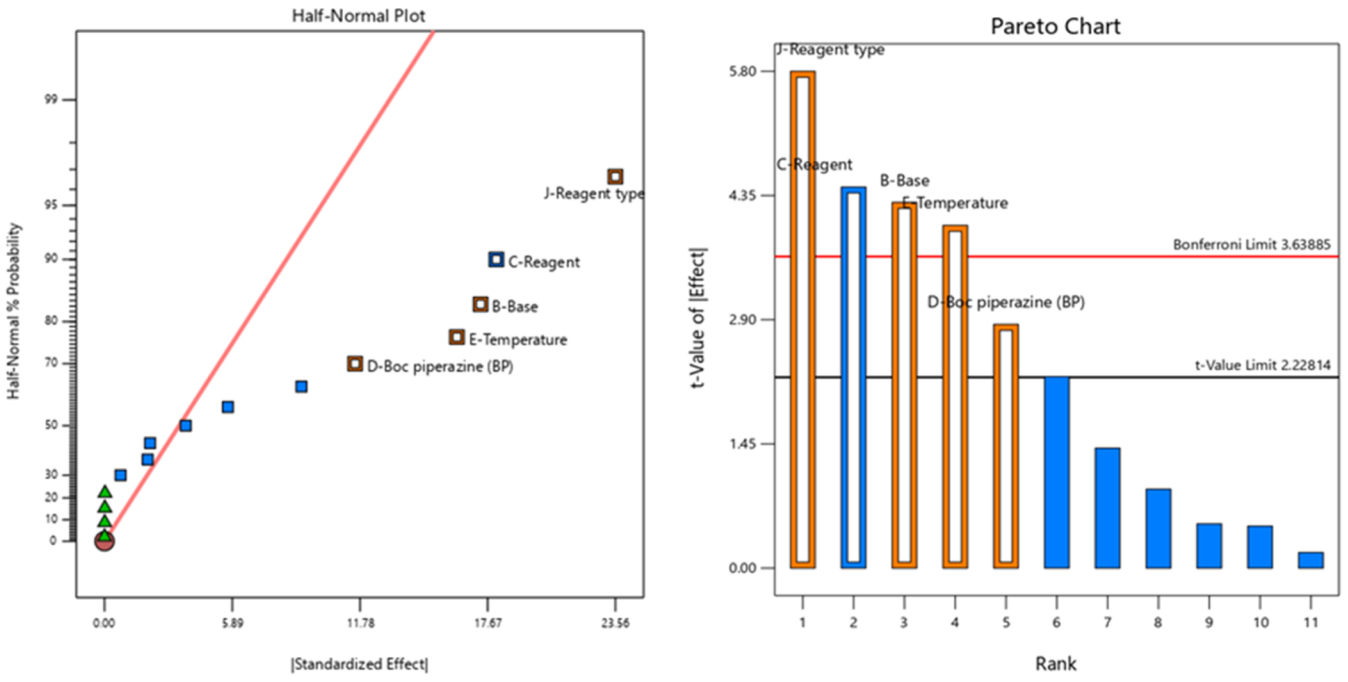

Figure 2. Half-normal plot and Pareto chart for the content of **2**.

stages. These identified KMAs and KPPs are later studied using the DoE trials to gain in-depth insights into the impact of changes in factors (KMAs and KPPS) on the desired responses. These KMAs and KPPs, whose variability impacts a CQA that should be monitored or controlled to ensure the process produces the desired quality, are called CMAs and CPPs, respectively. They are used to monitor the product throughout its life cycle.

Olaparib is a poly(ADP-ribose) polymerase (PARP) inhibitor[5] indicated to treat ovarian cancer, breast cancer, fallopian tube cancer, peritoneal cancer, pancreatic cancer, and prostate cancer. The PARP family of proteins is involved in the repair of single-strand DNA. PARP inhibition may lead to the accumulation of PARP-DNA complexes and single-strand breaks that give rise to double-strand DNA during DNA replication. These double-strand breaks may lead to DNA damage, potentiated by the loss of function of homologous recombination repair enzymes such as BRCA. The induced DNA damage may lead to the initiation of apoptotic pathways and cell death.

Synthesis of Olaparib **1** as shown in Figure 1 consists of three chemical conversions; 1. amidation, 2. deprotection, and 3. acylation (Scheme 1). In the first step, amidation features the coupling of 2-fluoro-5-((4-oxo-3,4-dihydrophthalazin-1-yl)-methyl)benzoic acid **2** with *tert*-butyl piperazine-1-carboxylate **3** in the presence of 2-(1*H*-benzotriazol-1-yl)-1,1,3,3-tetramethyluronium hexafluorophosphate (HBTU), coupling reagent, *N*,*N*-diisopropylethylamine (DIPEA) base, and dimethylacetamide (DMAc), solvent medium to obtain *tert*-butyl 4-(2-fluoro-5-((4-oxo-3,4-dihydrophthalazin-1-yl)methyl)benzoyl)-piperazine-1-carboxylate **4**, which upon deprotection of Boc group with aqueous hydrochloric acid in methanol medium

https://doi.org/10.1021/acsomega.4c01293
ACS Omega 2024, 9, 30327−30349

Table 3. ANOVA for Content of 2 Before Pooling[a]

source	sum of squares	df	mean square	*F*-value	*p*-value	
model	7084.91	9	787.21	11.67	0.0037	significant
A-solvent quantity	15.36	1	15.36	0.2276	0.6502	
B-base	1196.95	1	1196.95	17.74	0.0056	
C-reagent	1429.34	1	1429.34	21.18	0.0037	
D-boc piperazine	530.31	1	530.31	7.86	0.0310	
E-temperature	1069.47	1	1069.47	15.85	0.0073	
F-dilution of BP in solvent	125.49	1	125.49	1.86	0.2216	
G-solvent type	17.10	1	17.10	0.2535	0.6326	
H-base type	54.27	1	54.27	0.8042	0.4044	
J-reagent type	2203.29	1	2203.29	32.65	0.0012	
residual	404.85	6	67.48			
lack of fit	404.78	2	202.39	11 074.68	<0.0001	significant
pure error	0.0731	4	0.0183			
cor total	7489.77	15				

[a]Fit statistics R^2 = 0.9459, adjusted R^2 = 0.8649, and predicted R^2 = 0.0108.

Table 4. ANOVA for Content of 2 After Pooling[a]

source	sum of squares	df	mean square	*F*-value	*p*-value	
model	6850.61	5	1370.12	21.44	<0.0001	significant
B-base	1165.51	1	1165.51	18.24	0.0016	
C-reagent	1265.53	1	1265.53	19.80	0.0012	
D-boc piperazine	517.55	1	517.55	8.10	0.0174	
E-temperature	1023.40	1	1023.40	16.01	0.0025	
J-reagent type	2150.62	1	2150.62	33.65	0.0002	
residual	639.16	10	63.92			
lack of fit	639.08	6	106.51	5828.40	<0.0001	significant
pure error	0.0731	4	0.0183			
cor total	7489.77	15				

[a]Fit statistics R^2 = 0.9147, adjusted R^2 = 0.8720, and predicted R^2 = 0.7890.

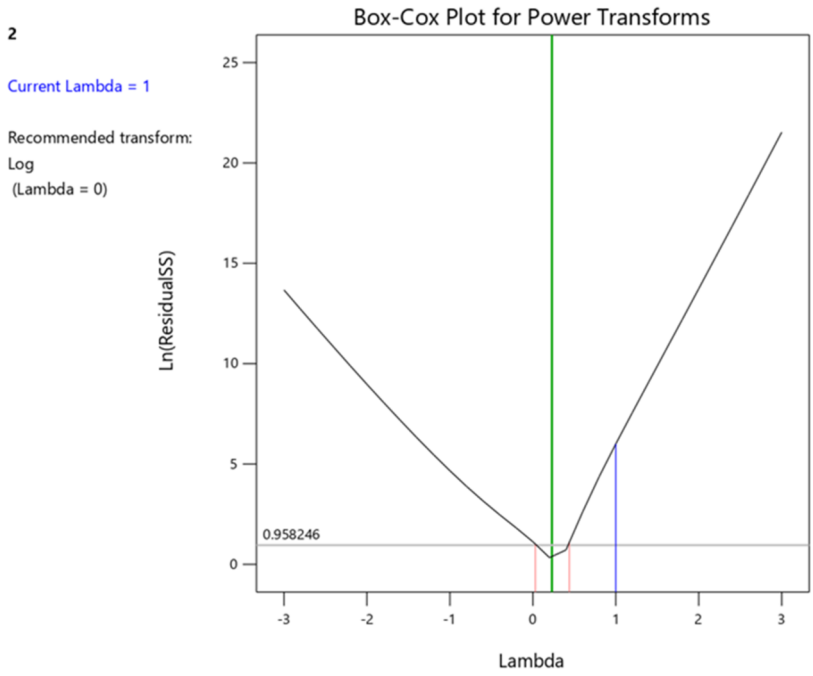

Figure 3. Box−Cox plot for the content of **2**.

forms 4-(4-fluoro-3-(piperazine-1-carbonyl)benzyl)phthalazin-1(2*H*)-one **5**. Thereafter, acylation was carried out with cyclopropane carbonyl chloride **6** in the presence of triethylamine (TEA) base and dimethylformamide (DMF), solvent offered Olaparib **1**.

This work focuses on QbD as a systematic risk-based approach to Olaparib **1** (API) development, manufacturing,

https://doi.org/10.1021/acsomega.4c01293
ACS Omega 2024, 9, 30327−30349

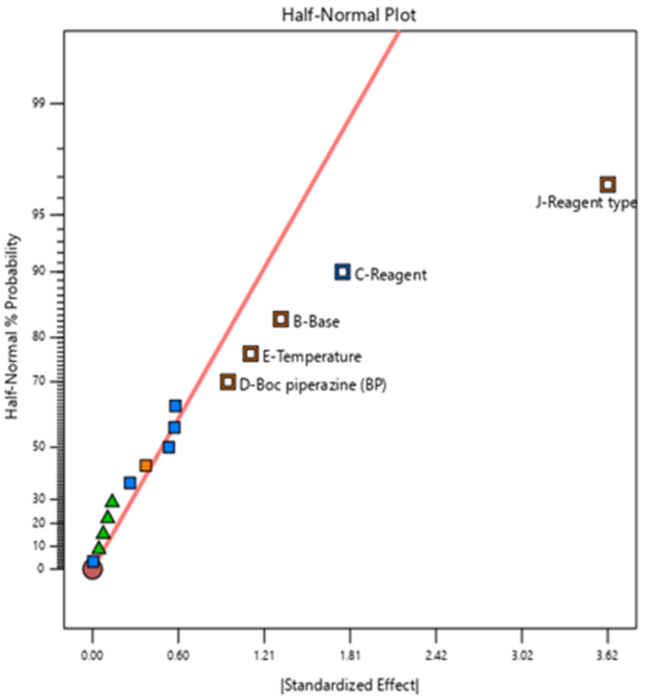

Figure 4. Half-Normal Plot for the Content of **2** (Natural Logarithmic Transformation).

and lifecycle management. Each of the three chemical transformations was separately studied by employing QbD principles and optimized using the design of experiments (DOE)[6−10] to achieve maximum reaction conversion, excellent chemical purity, and isolated yield.

MATERIALS AND METHODS

Key starting materials **2**, **3**, and **6** were purchased from commercial suppliers (>98%) and used as is, 1-[bis-(dimethylamino)methylene]-1*H*-benzotriazolium-3-oxide hexafluorophosphate (HBTU) was purchased from Molekula biokemix (>99%, product no 87448736), and triethylamine (TEA), *N*,*N*-dimethylformamide (DMF), *N*,*N*-dimethylacetamide (DMAc), methanol (MeOH), hydrochloric acid (HCl, 37%), and aqueous ammonia (NH_3, 25%) were purchased from commercial suppliers. Aqueous solutions were prepared using ultrapure Milli-Q distilled water (Millipore, Bedford, MA).

The high-performance liquid chromatography (HPLC) method was developed for the analysis of process-related impurities and degradation products of Olaparib. The chromatographic analysis was performed on a Waters Alliance 2695 series instrument (Waters Corporation). The system is composed of a quaternary gradient pump (QSM), an auto sampler (sample manager SM), and a column oven, with a PDA detector and Empower3 software were utilized for process monitoring and data acquisition. The chromatographic column of YMC pack ODS A (150 mm × 4.6 mm, 3.0 μ) was used in the present work for the desired separation. The injection volume used was 10.0 μL, and the column temperature was set to 30 °C; the analytes were detected in a photodiode array detector at 220 nm.

^{1}H and ^{13}C NMR spectra were recorded on a Bruker Avance 400 and 100 MHz spectrometer, respectively, in DMSO-d_6, CD_3OD, and $CDCl_3$. All chemical shifts (δ) were reported in parts per million (ppm) and referenced to residual protium or the carbon resonance of the NMR solvent, respectively. The following abbreviations were used to designate chemical shift multiplicities: s, singlet; d, doublet; t, triplet; q, quartet; m, multiplet; br, broad; and brs, broad singlet. Mass spectra were recorded by using electrospray ionization (ESI). FT-IR spectra were recorded on a PerkinElmer model spectrum series FT-IR as KBr pellet.

Design of Experiments is a scientific, efficient method for designing and analyzing a series of experiments to study the relationship between multiple input variables (independent variables) and key output variables (dependent variables).[16] It is a structured multivariate experimental approach for collecting data and making data-driven decisions. DoE is a superior methodology over the best-guess approach and the one-factor-at-a-time (OFAT) approach. The best-guess approach has at least two disadvantages.[16] First, suppose that the initial best guess does not produce the desired results. Now the experimenter has to take another guess at the correct combination of factor levels. This could continue for a long time without any guarantee of success. Second, suppose that the initial best guess produces an acceptable result. Now the experimenter is tempted to stop testing, although there is no guarantee that the best solution has been found. Another strategy of experimentation that is used extensively in practice is the OFAT approach. The OFAT method consists of selecting a starting point or baseline set of levels for each factor and then successively varying each factor over its range with the other factors held constant at the baseline level. The major disadvantage of the OFAT strategy is that it fails to consider any possible interaction between the factors. An interaction is the failure of one factor to produce the same effect on the response at different levels of another factor.[16]

Table 5. ANOVA for Content of 2 after Pooling (Natural Logarithmic Transformation)[a]

source	sum of squares	df	mean square	*F*-value	*p*-value	
model	87.80	5	17.56	22.04	<0.0001	significant
B-base	6.80	1	6.80	8.54	0.0153	
C-reagent	11.99	1	11.99	15.05	0.0031	
D-boc piperazine	3.52	1	3.52	4.42	0.0619	
E-temperature	4.79	1	4.79	6.01	0.0341	
J-reagent type	50.91	1	50.91	63.89	<0.0001	
residual	7.97	10	0.7967			
lack of fit	5.98	6	0.9965	2.00	0.2609	not significant
pure error	1.99	4	0.4971			
cor total	95.77	15				

[a]Fit statistics R^2 = 0.9168, adjusted R^2 = 0.8752, and predicted R^2 = 0.7751.

https://doi.org/10.1021/acsomega.4c01293
ACS Omega 2024, 9, 30327−30349

Table 6. ANOVA for the Yield After Pooling[a]

source	sum of squares	df	mean square	*F*-value	*p*-value	
model	12 301.69	6	2050.28	176.40	<0.0001	significant
B-base	2302.74	1	2302.74	198.12	<0.0001	
C-reagent	1507.32	1	1507.32	129.68	<0.0001	
D-boc piperazine (BP)	160.82	1	160.82	13.84	0.0048	
E-temperature	2368.80	1	2368.80	203.80	<0.0001	
H-base type	316.44	1	316.44	27.23	0.0006	
J-reagent type	3975.06	1	3975.06	342.00	<0.0001	
residual	104.61	9	11.62			
lack of fit	97.02	5	19.40	10.23	0.0214	significant
pure error	7.59	4	1.90			
cor total	12 406.30	15				

[a]Fit statistics R^2 = 0.9916, adjusted R^2 = 0.9859, and predicted R^2 = 0.9653.

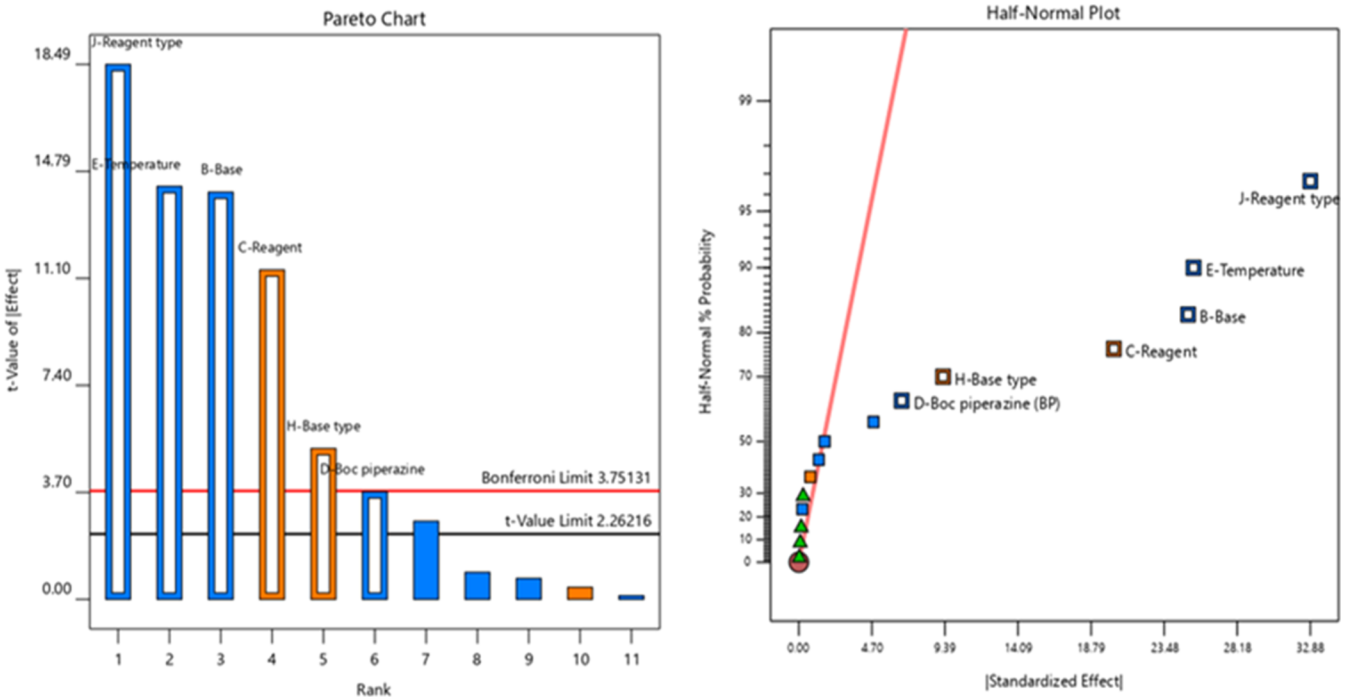

Figure 5. Pareto chart and half-normal plot for % yield.

Table 7. Summary of Screening Experiments

parameter	screening		optimization DOE	
solvent type	DMAc and NMP		DMAc	
reagent type	HBTU and EDC·HCl/HOBt·H_2O		HBTU	
base type	TEA and DIPEA		TEA	
DMAc vol for reaction	3	12	7 vol	
DMAc vol for dilution of boc piperzine	3	6	5 vol	
boc piperazine equiv	1.0	2.0	1.0	1.5
HBTU equiv	1.0	2.0	1.0	1.4
TEA equiv	1.0	3.0	1.0	2.0
reaction temperature (°C)	10	40	0	20

The Design of Experiments was developed to consider all possible interactions between variables compared with the traditional OFAT approach. DoE manipulates each process variable individually to identify invisible links among them, including main, two-way, and three-way interactions.[18] There are many types of experimental designs that can be applied throughout the workflow to establish and control the CPPs. The choices of design should be fit for the intended purpose. A screening design can then be used to filter the vital few parameters affecting the process from the many tested, while an optimization design generates a more detailed understanding of the cause-and-effect relationships between these key parameters and the process attributes. The resulting models at this stage can be used to predict the most favorable conditions and establish predicted acceptable ranges or edge of failure boundaries, and

https://doi.org/10.1021/acsomega.4c01293
ACS Omega 2024, 9, 30327−30349

Table 8. Design Layout Including Experimental Results

run	A: boc piperazine (equiv)	B: HBTU (equiv)	C: TEA (equiv)	D: reaction temperature (°C)	2 (%)	4 (%)
1	1.20	1.21	1.00	12	0.13	97.35
2	1.36	1.40	2.00	5	0.46	95.95
3	1.50	1.00	1.00	20	1.69	95.77
4	1.32	1.00	1.36	7	3.46	93.76
5	1.50	1.00	2.00	0	7.15	90.36
6	1.35	1.02	2.00	20	0.34	95.77
7	1.00	1.17	1.51	10	0.95	94.70
8	1.50	1.25	1.00	10	0.14	97.29
9	1.00	1.00	1.00	0	4.20	93.47
10	1.50	1.40	1.00	0	0.03	97.73
11	1.50	1.21	1.61	12	0.40	96.26
12	1.36	1.40	1.27	20	0.22	96.36
13	1.20	1.21	1.59	0	0.20	96.76
14	1.50	1.21	1.61	12	0.40	96.29
15	1.20	1.21	1.59	0	0.18	97.12
16	1.00	1.32	2.00	20	1.72	89.97
17	1.00	1.02	2.00	6	2.62	94.24
18	1.00	1.40	1.26	5	0.19	97.22
19	1.18	1.38	1.64	13	0.66	94.71
20	1.32	1.00	1.36	7	3.85	93.61
21	1.20	1.21	1.00	12	0.12	97.08
22	1.00	1.02	1.29	20	1.55	95.61

Table 9. ANOVA for Content of 2[a]

source	sum of squares	df	mean square	*F*-value	*p*-value	
model	69.50	9	7.72	142.20	<0.0001	significant
A-boc piperazine	0.1892	1	0.1892	3.48	0.0866	
B-HBTU	21.77	1	21.77	400.97	<0.0001	
D-reaction temperature	3.67	1	3.67	67.66	<0.0001	
AB	2.69	1	2.69	49.56	<0.0001	
AD	5.56	1	5.56	102.41	<0.0001	
BC	0.6804	1	0.6804	12.53	0.0041	
BD	14.35	1	14.35	264.33	<0.0001	
A^2	1.72	1	1.72	31.59	0.0001	
B^2	8.95	1	8.95	164.85	<0.0001	
residual	0.6516	12	0.0543			
lack of fit	0.5757	8	0.0720	3.79	0.1067	not significant
pure error	0.0759	4	0.0190			
cor total	70.15	21				

[a]Fit statistics R^2 = 0.9907, adjusted R^2 = 0.9837, and predicted R^2 = 0.9540.

ultimately a risk-assessed design space within which to successfully operate the process.[19]

From various types of DoE designs, Plackett−Burman design (PBD), full factorial design (FFD), and I-Optimal designs were used based on the objective. PBD is a screening design used to determine significant factors affecting the process. FFD studies all of the possible combinations of input variables and their respective range of values.[16] Optimal designs are response surface designs (RSM)[17] used to estimate the quadratic effects along with the main effects and interaction effects. The effects of all process variables were investigated by using a stepwise linear model. The ANOVA method was applied to identify the power factors by calculating the *p*-value, *F* ratio, and *R* square (R^2).[18]

The *P*-value represents a probability that ranges between zero and one and is used to evaluate the significance of each variable. Variables with a *p*-value less than 0.05 (level of significance) have a high effect.[16] The *F* ratio measures the variance of the data around its mean. Consequently, the smaller the *p*-value and the higher the *F* ratio, the more significant is the variable. The mean square represents an estimate of population variance, while the sum of squares measures the variation of all observations from their mean.[16]

RESULTS AND DISCUSSION

Process Optimization Study of Amidation Step. The yield and purity of the amidation step, as presented in the synthetic Scheme 2, were reported to be 78 and 87%, respectively.[11−13] The optimization study aims to enhance the reaction conversion to more than 99% through a structured QbD approach with risk assessment, screening, and optimization.

A risk assessment based on the initial knowledge was carried out on the material attributes, process parameters involved in this reaction step, and their influence on the reaction yield and purity. From the risk assessment, KMAs such as coupling reagent and its equiv, base type and its equiv, solvent type and its

https://doi.org/10.1021/acsomega.4c01293
ACS Omega 2024, 9, 30327−30349

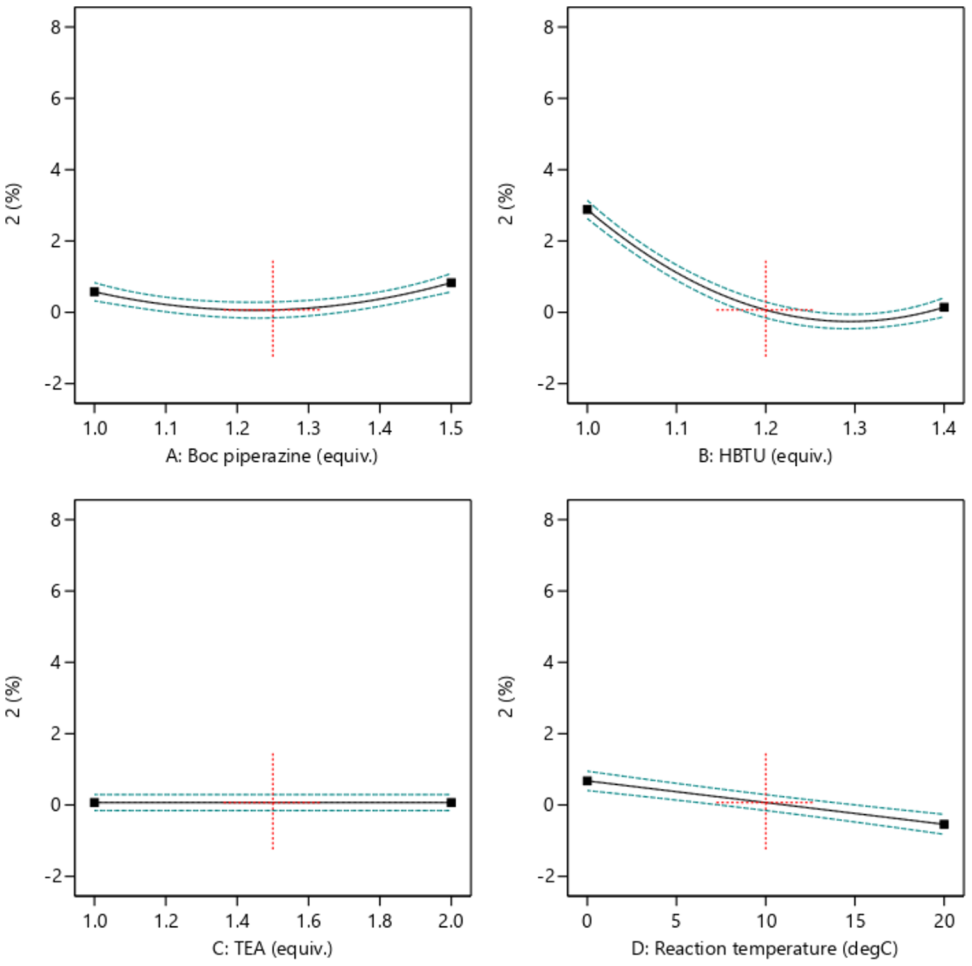

Figure 6. Individual effects plot for the content of **2**.

volume, Boc piperazine (BP) equiv, and KPPs such as temperature (Table 1) were identified as impacting attributes on the yield and purity. As per preliminary experimental data, reaction time remained constant for two h, even though reaction mass samples were collected in two time intervals (2 and 4 h). They were further taken into consideration in the design of the screening study design. Overall, three categorical factors and six continuous factors were taken into account for the screening study. Plackett−Burman *L*12 design with four replicate points was used for the study.

Design Layout and Experimental Results. Postscreening experimentation, % reaction conversion in terms of % content of **2** was measured using high-performance liquid chromatography (HPLC) by the area normalization method. The data showed that the % content of **2** (unreacted starting material) varied from 0.06 to 63.65% (Table 2). All of the screening experiments proceeded for isolation and yields after calculating purity correction. Yield (%) ranged from 11.6 to 94.6% (Table 2). Responses obtained were subjected to analysis to identify the vital factors from the various trivial KMAs and KPPs that would impact the final attributes, i.e., % content of **2** and % yield.

Statistical Analysis for % Content of 2. Design of Experiments analysis, based on the half-normal plot, Pareto chart (Figure 2), and *p*-value (<0.05) of the ANOVA statistics (Table 3), type of reagent, reagent quantity, base quantity, reaction temperature, and Boc piperazine quantity were found to be significant factors.

For the selected model, the predicted R^2 and adjusted R^2 were found to be 0.0108 and 0.8649, respectively. A difference of more than 0.2 indicates a large block effect or a potential problem with the model or data or both.[14] Model refinement, transformation of response, and removal of outliers can be considered a credible way to improve the model.[14]

In this case, the model refinement was performed by eliminating not-significant (*p*-value >0.05) factors from the model. From the ANOVA (Table 3), *p*-values for factors A−H were more than 0.05, hence removed from the model. Insignificant factors eliminated during model refinement would be added to the error term enabling the power of detection and, in turn, increasing the estimation accuracy. Postmodel refinement (Table 4) predicted that R^2 drastically increased from 0.0108 to 0.7890, which is in reasonable agreement with the adjusted R^2 of 0.8720. However, the lack of fit test was still significant even after model refinement. In case a lack of fit test is significant, it does not necessarily mean the model is poor. The cause of a significant lack of fit test result is the existence of a curvature or an extremely small error. Arguably, in this case, the pure error was extremely small. In addition to the lack of fit test and pure error, the Box−Cox plot (Figure 3) suggested a logarithmic transformation. We analyzed the % content of **2** data by transformation of the variables.

The data of % content of **2** were transformed into a natural logarithm and then analyzed again. Half-normal plot (Figure 4) and ANOVA statistics (Table 5) revealed that reagent type

https://doi.org/10.1021/acsomega.4c01293
ACS Omega 2024, 9, 30327−30349

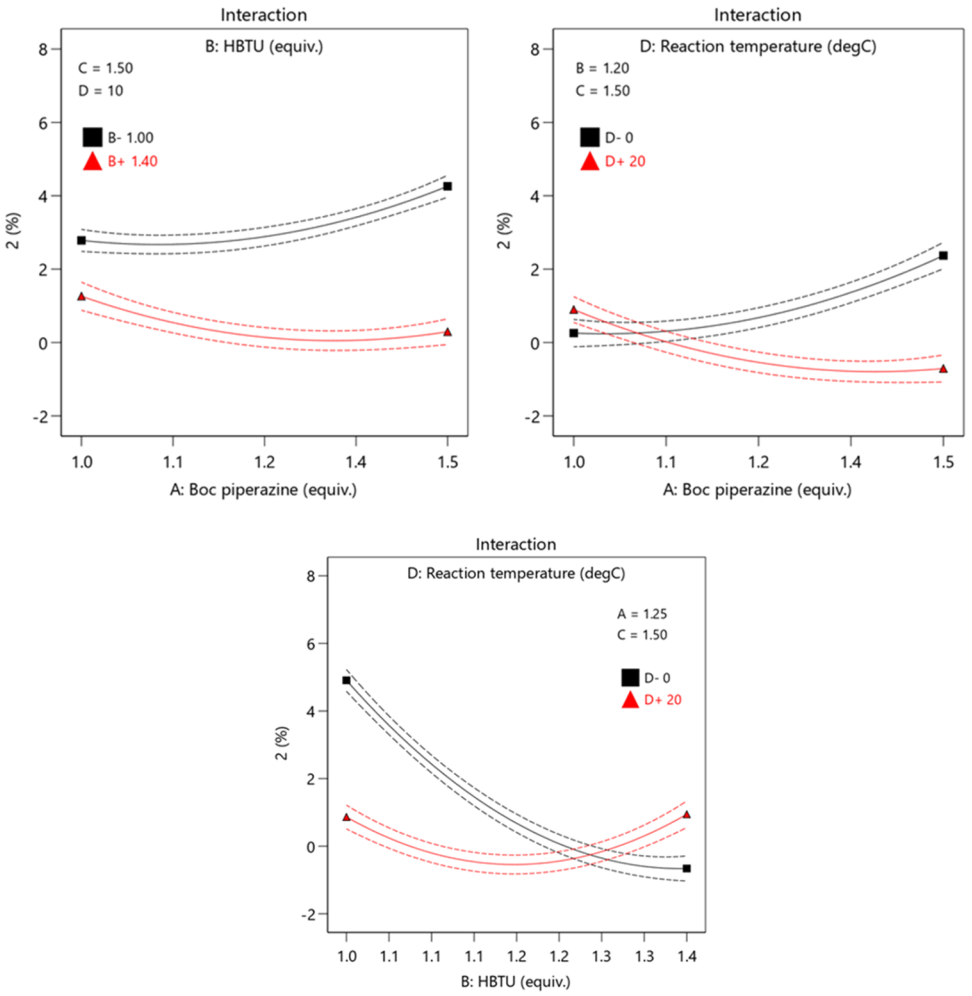

Figure 7. Interaction effect plots for the content of **2**.

contributed to the % content of **2** to a great extent, along with a contribution from the reagent quantity, base quantity, reaction temperature, and Boc piperazine quantity. The results of the lack of fit test were now not significant. It is reasonable to conclude that the model analyzed by variable transformation is more appropriate than that analyzed without variable transformation.

Based on a half-normal plot (Figure 4), reagent type has a strong positive effect (p-value 0.0002) (HBTU preferable over EDC·HCl) to minimize the content of **2**, reagent quantity has a negative effect, base quantity has a positive effect, and reaction temperature has a positive effect.

Statistical Analysis for % Yield. For % yield, upon analysis of results (after correction for purity), it was found that based on the p-value (<0.05) of ANOVA statistics, reagent type, reaction temperature, base quantity, reagent quantity, base type, and BOC piperazine quantity were significant factors (Table 6). The lack of fit test was also significant due to the small pure error observed.

The predicted R^2 of 0.9653 was in reasonable agreement with the adjusted R^2 of 0.9859. Based on a half-normal plot and Pareto chart (Figure 5), base quantity has a negative effect, reagent quantity has a positive effect, reaction temperature has a negative effect, and base type has a positive effect (TEA as a base is preferable when compare to DIPEA to maximize the yield), and reagent type has a strong negative effect (HBTU as reagent gives higher yields).

Inferences from Screening Design and Way Forward. From the outcome of the screening design, factors like solvent type, solvent quantity, and BP dilution solvent quantity were nonsignificant and had minimal or negligible impact on the reaction process. These factors, irrespective of their factor levels, did not impact much and were fixed based on practical experience, cost of material, and ease of processing. Hence, DMAc as a solvent and solvent quantity at 7 vol and BP dilution solvent quantity at 5 vol were selected. Furthermore, two categorical factors were observed as significant, namely reagent type and base type, for achieving the target of maximum reaction conversion (reduced % content of **2**) and % yield. Of the categorical factors, HBTU as a reagent and TEA as a base give higher % yields and lower content of **2**. Hence, HBTU and TEA were finalized as reagents and bases for further use in the reaction process and optimization studies.

Additionally, four continuous factors, which are process parameters (Reagent quantity, base quantity, BP quantity, and temperature), were found to be significant for impact on responses (reaction conversion and % yield) and are referred to as CMAs and CPPs henceforth and considered in the optimization study. The factors and their levels considered for the optimization study are shown in Table 7. Factor levels were revised based on the directional inputs from the screening design.

https://doi.org/10.1021/acsomega.4c01293
ACS Omega 2024, 9, 30327−30349

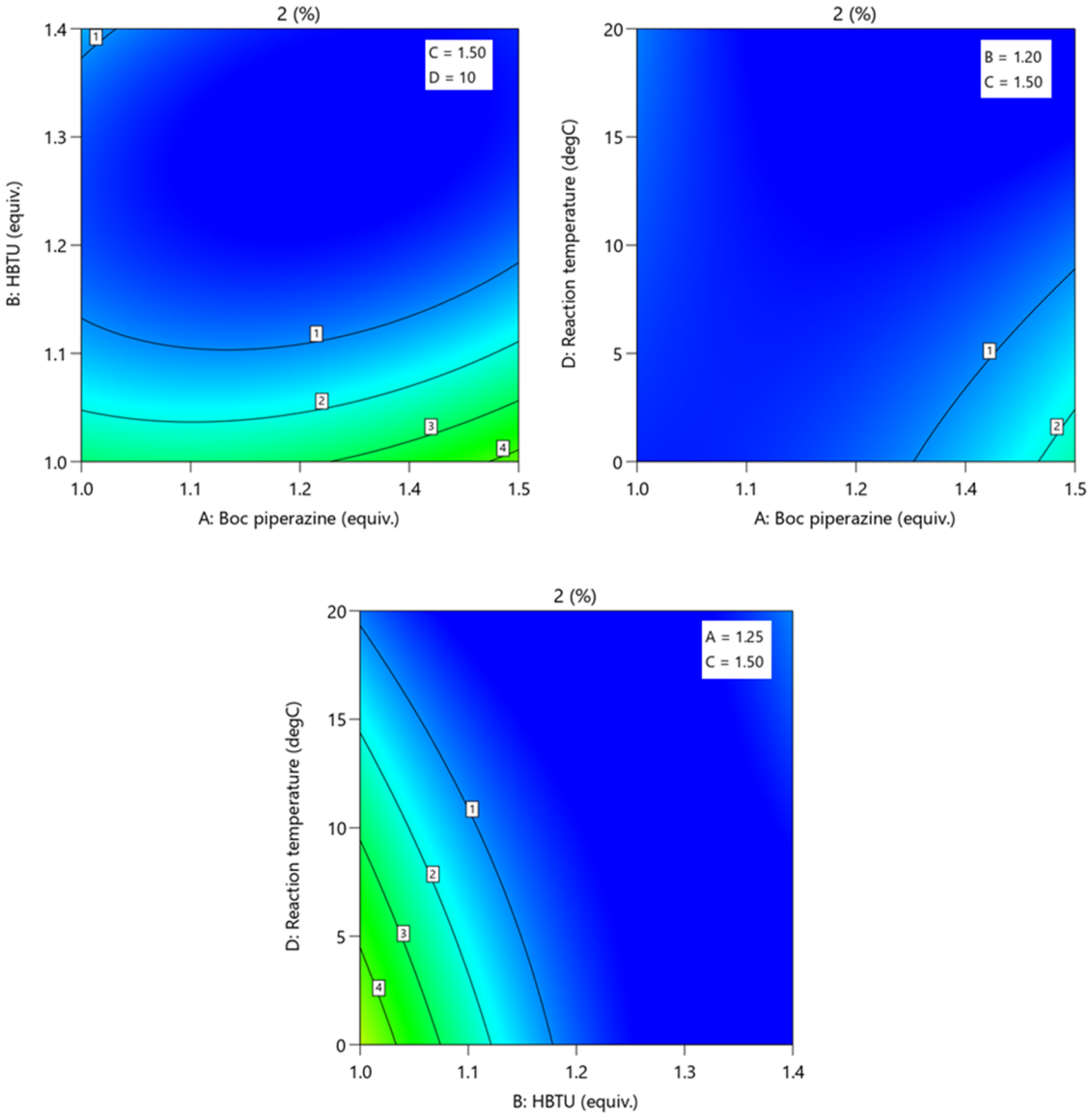

Figure 8. Contour plots for content of **2**.

Optimization DoE studies are carried out to study the in-depth effect of the factors, that is, the two-factor interaction (2FI) effect and nonlinear behavior of the factors, which were not estimated in the screening phase. This study will help to achieve a higher precision in predicting the outcome. Among the response surface designed, an I-Optimal design with a quadratic model, 4 replicates, and 3 lack of fit points was selected (Table 8). A pure error was estimated from replicate data points, and the lack of fit points was used to fit the higher-order model. Data from the model point will be used to estimate the main effects of the factors, 2FI and quadratic effects.

Statistical Analysis for % Content of 2. The HPLC results of the % content of **2** were subjected to statistical analysis. As per the output of DoE analysis, three main effects, four 2FI, and two quadratic effects were significant (Table 9), and the result of the lack of fit test was nonsignificant. As can be seen from the figure of individual effects plot, interaction effects plot, and ANOVA statistics, the parameters that greatly affect reaction % content of **2** were found to be Boc piperazine equiv, HBTU equiv, and reaction temperature (Figure 6), along with 2FI between boc piperazine and HBTU equiv, boc piperazine and reaction temperature, HBTU equiv, TEA equiv, HBTU equiv, and reaction temperature (Figure 7). The predicted R^2 of 0.9540 is in reasonable agreement with the adjusted R^2 of 0.9837, indicating that the model is sufficient to explain the effect of factors on response and almost 98% of the variation in the given data.

The final regression equation in terms of coded factors for the content of **2** are as follows;

$$\begin{aligned}\text{content of } \mathbf{2}(\%) = {} & 0.0683 + 0.1267 \times A - 1.37 \times B \\ & - 0.6092 \times D - 0.6108 \times AB \\ & - 0.9298 \times AD + 0.3115 \times BC \\ & + 1.41 \times BD + 0.6364 \times A^2 \\ & + 1.45 \times B^2\end{aligned}$$

This equation is coded factors and can be used to predict the response for given levels of each factor. By default, the high level of the factors is coded as +1, and the low level is coded as −1. It is also useful for identifying the relative impact of the factors by comparing the factor coefficients.

https://doi.org/10.1021/acsomega.4c01293
ACS Omega 2024, 9, 30327−30349

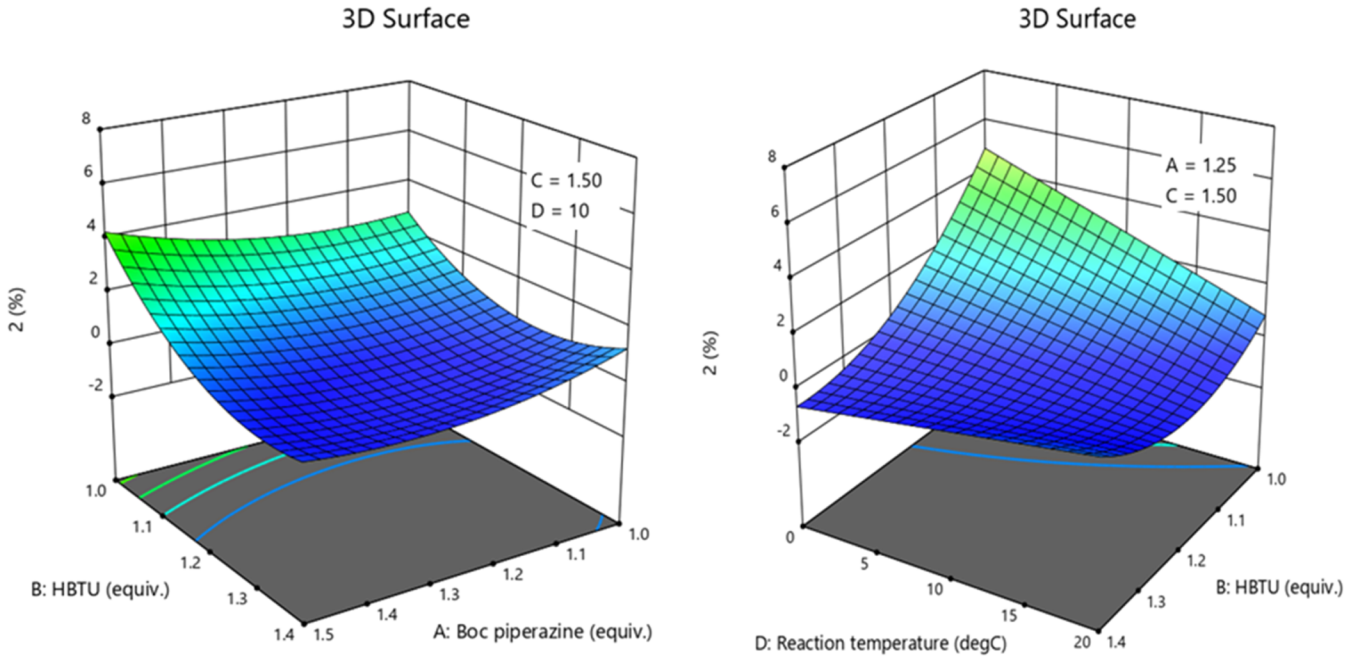

Figure 9. 3D surface plot for the content of **2**.

Table 10. ANOVA for Content of 4[a]

source	sum of squares	df	mean square	*F*-value	*p*-value	
model	90.18	10	9.02	147.23	<0.0001	significant
A-boc piperazine	3.88	1	3.88	63.36	<0.0001	
B-HBTU	3.35	1	3.35	54.73	<0.0001	
C-TEA	4.62	1	4.62	75.51	<0.0001	
AB	16.67	1	16.67	272.24	<0.0001	
AD	7.12	1	7.12	116.17	<0.0001	
BC	2.38	1	2.38	38.86	<0.0001	
BD	19.26	1	19.26	314.44	<0.0001	
CD	2.18	1	2.18	35.58	<0.0001	
A^2	7.15	1	7.15	116.81	<0.0001	
B^2	8.83	1	8.83	144.17	<0.0001	
residual	0.6737	11	0.0612			
lack of fit	0.5635	7	0.0805	2.92	0.1585	not significant
pure error	0.1102	4	0.0276			
cor total	90.85	21				

[a]Fit statistics R^2 = 0.9926, adjusted R^2 = 0.9858, and predicted R^2 = 0.9464.

The interaction plot, contour graph, and 3D surface plot (Figures 7−9) reveal that moderate Boc piperazine equiv, moderate to higher HBTU equiv, and moderate to high reaction temperature favors toward lower unreacted starting material, i.e., % content of **2**.

Statistical Analysis for Content of 4. Post analysis of the levels of Compound **4**, the data were subjected to statistical analysis. According to the result, three main effects, five 2FI, and two quadratic effects were significant (Table 10), and the lack of fit test was insignificant. As can be seen from individual effects plots, interaction effects plot. and ANOVA statistics, the parameters that greatly affect the content of **4** were found to be Boc piperazine equiv, HBTU equiv, and TEA equiv (Figure 10) along with 2FI between Boc piperazine equiv, HBTU equiv, TEA equiv, and reaction temperature (Figure 11). The interaction plot and contour graph (Figures 11 and 12) reveal that moderate Boc piperazine equiv, moderate to higher HBTU equiv, lower to moderate TEA equiv, and moderate to high reaction temperature favor higher product formation (content of **4**).

The predicted R^2 of 0.9464 is in reasonable agreement with the adjusted R^2 of 0.9858. The statistical analysis without variable transformation is appropriate for the data of the content of **4** to conclude that the model is sufficient to explain the effect of factors on the response and almost 98% of the variation in the given data.

The final regression equation in terms of coded factors for the content of **4** was as follows:

$$\begin{aligned}\text{content of } \mathbf{4}(\%) = {} & 96.72 + 0.5934 \times A + 0.5465 \times B \\ & - 0.6805 \times C + 1.55 \times AB \\ & + 1.08 \times AD - 0.5839 \times BC \\ & - 1.62 \times BD - 0.5952 \times CD \\ & - 1.30 \times A^2 - 1.44 \times B^2\end{aligned}$$

https://doi.org/10.1021/acsomega.4c01293
ACS Omega 2024, 9, 30327−30349

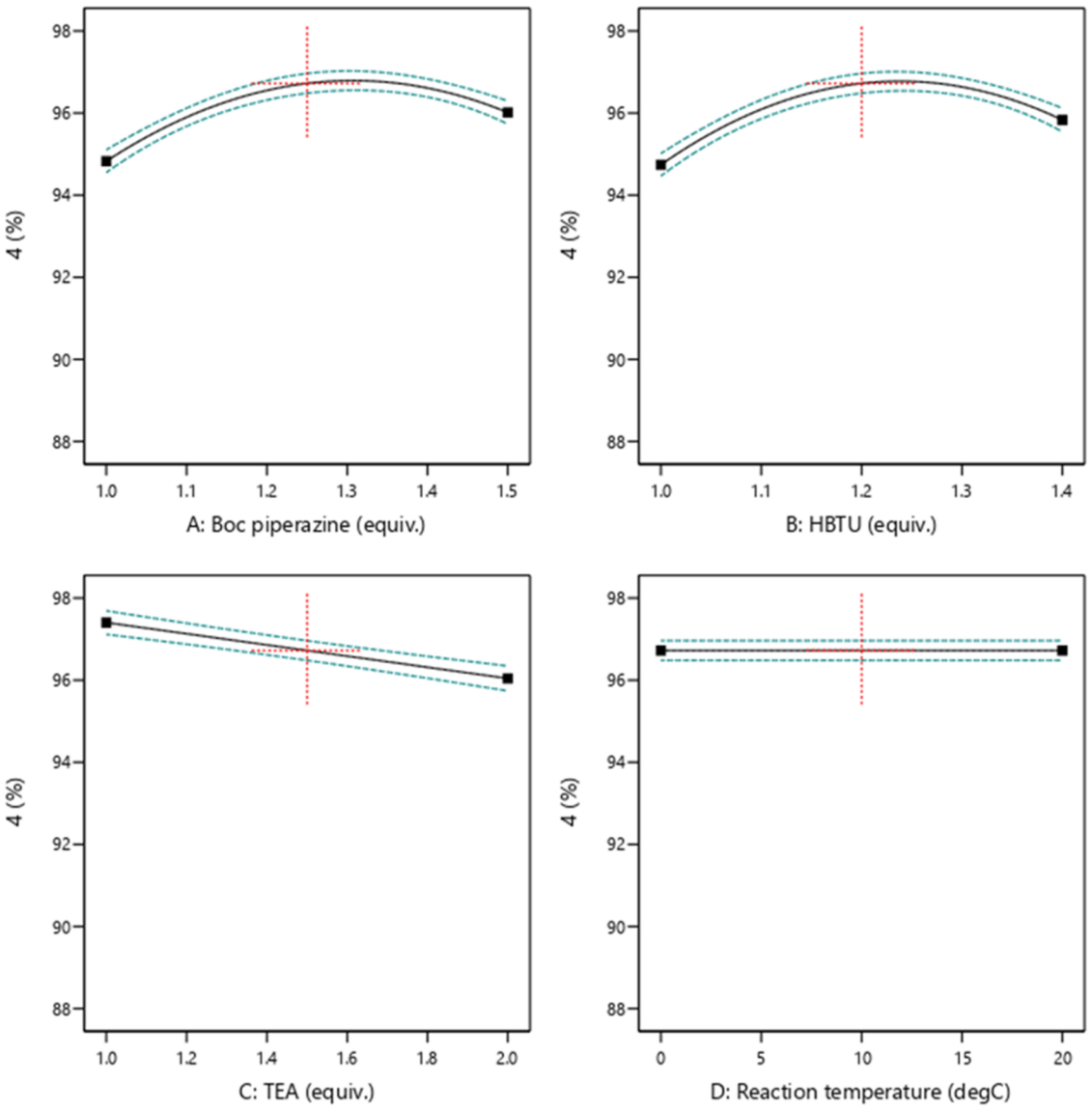

Figure 10. Individual effects plot for content of **4**.

Constructing Design Space for Content of 2 and 4. Design space was constructed by keeping the criteria of unreacted starting material (content of **2**) as NMT 1% and required product (content of **4**) as NLT 96% (Figure 13). Based on these criteria, acceptable ranges for each factor were derived (Table 11). Design space was verified by conducting additional experiments.

The yellow region in the diagram is the sweet zone or the operating zone/design space. Inside the yellow zone, the reaction process can be operated anywhere to meet the defined product specifications/criteria.

Summary for Amidation Step. Quality by design concepts were applied to enhance the reaction conversion and selectivity by identifying critical factors (screening design) and optimizing the factor settings (RSM design). A robust process setting was identified, and through selective control of ranges of CMAs and CPPs such as Boc piperazine equiv, HBTU equiv, TEA equiv, and reaction temperature, design space was defined to obtain more than 99% reaction conversion and 96% selectivity.

After ensuring more than 99% reaction conversion, the reaction process was further optimized to isolate the product (content of **4**) to more than 99% purity and 90% yield by controlling factors like methanol quantity, water quantity, heating/cooling rate, and temperature.

Optimization Study of Deprotection Step. As per the reported literature, the Boc group was removed in aq ethanolic HCl to provide free amine **5** (Scheme 3). In optimization, ethanolic HCl was replaced with aq. HCl and methanol as a solvent medium. Based on risk assessment, factors like the quantity of aq. HCl, methanol, and reaction temperature were studied to maximize the product (% content of **5**), minimize the initial reactant (% content of **4**), and minimize degradation impurity (% content of **2**). To check the reaction profile over time, reaction mass samples were collected after 2, 6, and 10 h. There was no major progress observed after 2 h.

Since there were only three factors to be studied, a full factorial design with two center points was selected, and the full factorial design gives the number of runs equal to 2^n. For studies with a lesser number of factors, a full factorial design would make a better choice, as the design would give the whole idea of main effects, all 2FI and 3FI model effects. As the number of factors increases, the design becomes cumbersome, as the number of

https://doi.org/10.1021/acsomega.4c01293
ACS Omega 2024, 9, 30327−30349

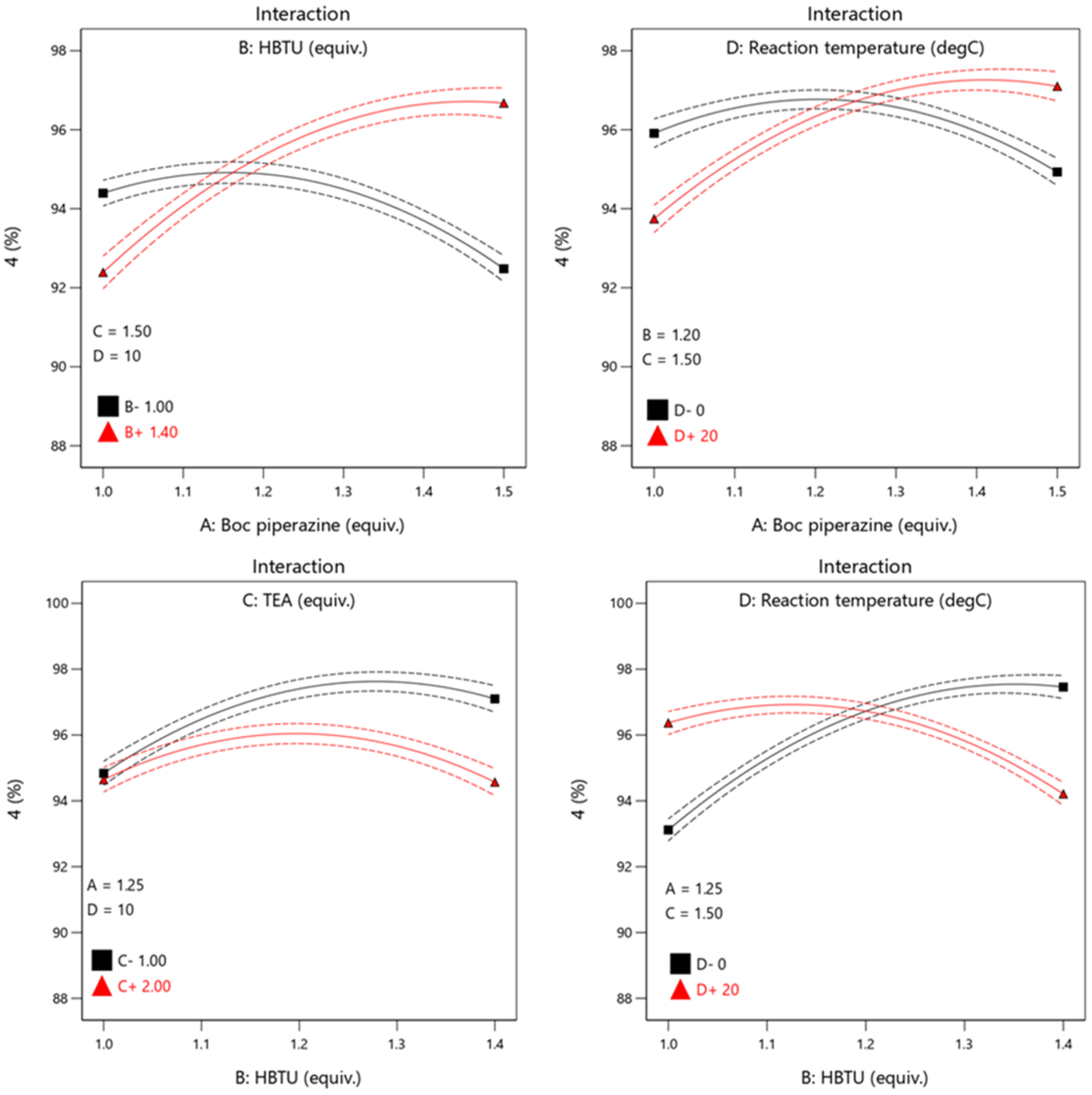

Figure 11. Interaction Effect Plots for the content of **4**.

runs swells drastically. The duplicate center point would help to measure the error between the experiments due to lurking variables. Lurking variables are the factors that are unknown and unavoidable but may impact your response. The factors and their levels considered for the study are represented in Table 12.

Experimental Results and Statistical Analysis. After conducting experiments, reaction conversion (content of **4**), formation of required product **5**, and degradation impurity of **2** were measured by HPLC by area normalization. The data demonstrated that the content of **4** (unreacted starting material) varied from 0.03 to 95.77%, the content of **5** varied from 2.33 to 96.58%, and the content of **2** varied from 0.03 to 6% (Table 13). The data covered almost the entire range for the reactant and the product content, indicating good coverage of response. This benefits a better understanding of the impact of factors studied on response. All of the responses were analyzed to identify significant factors responsible for the variation.

Statistical Analysis for Unreacted Starting Material Content 4. Analysis results based on the half-normal plot, Pareto chart (Figure 14), and *p*-value (<0.05) of the ANOVA statistic (Table 14) showed that of the studied models, only the main effect, which is reaction temperature, had a significant negative effect on unreacted starting material content **4**. Also, the lack of fit test was found to be nonsignificant. It could be inferred from the data that a higher temperature is preferable to minimize the unreacted starting material content of **4** in the reaction. The model adequately explains the variation observed in the data, as the predicted R^2 of 0.9736 is in reasonable

https://doi.org/10.1021/acsomega.4c01293
ACS Omega 2024, 9, 30327−30349

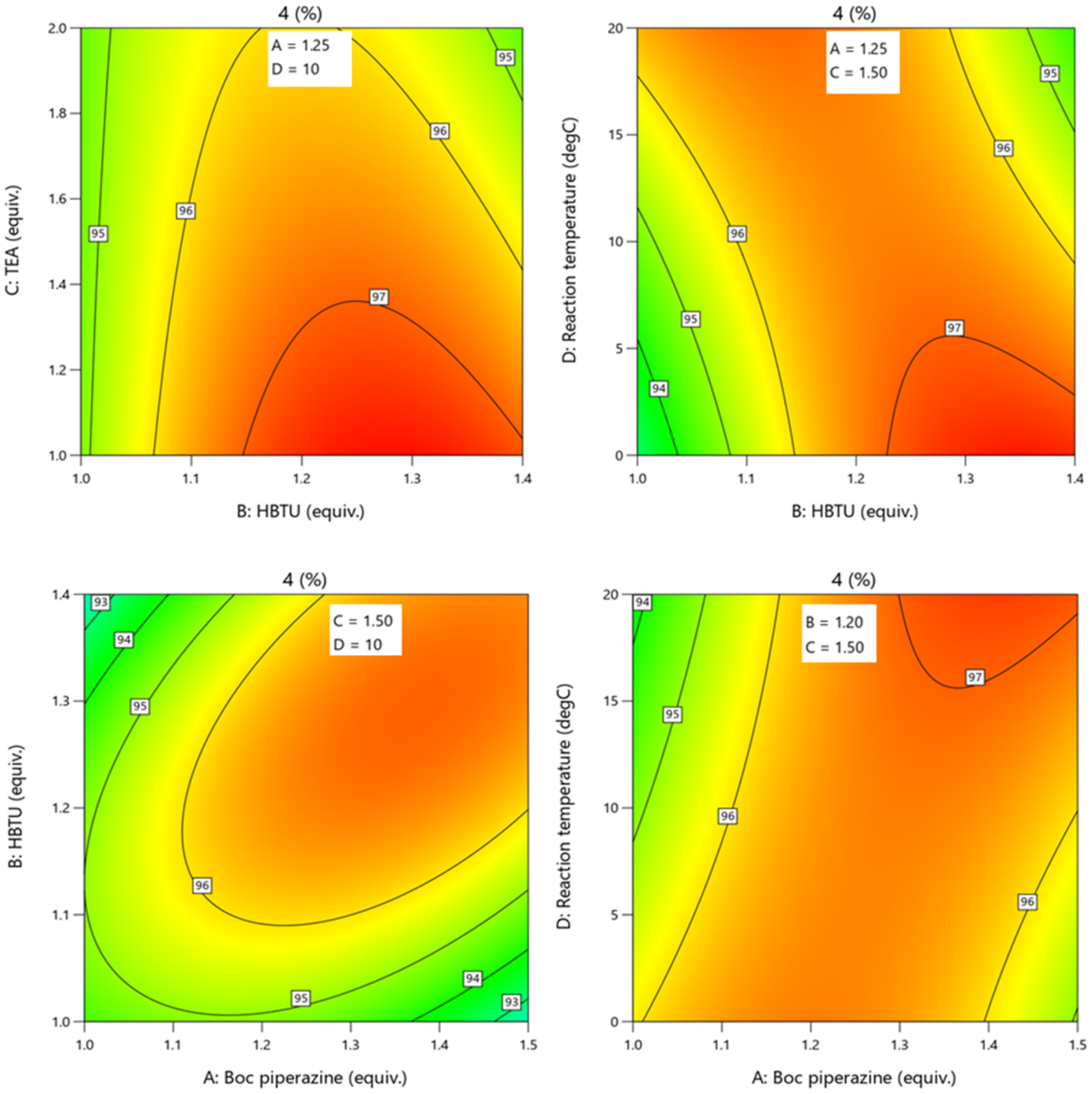

Figure 12. Contour plots for the content of **4**.

agreement with the adjusted R^2 of 0.9785. Almost 97% of the change in the response is explained by the effect of temperature.

The final regression equation in terms of coded factors for the content of **4** was as follows:

$$\text{content of } \mathbf{4}(\%) = +48.63 - 46.08 \times \text{C}$$

Statistical Analysis for Required Product Content 5. Like the analysis of the unreacted starting material content **4**, analysis results for product content **5** showed that based on the half-normal plot, Pareto chart (Figure 15) and *p*-value (<0.05) of the ANOVA statistic (Table 15) of the studied models, only main effect, reaction temperature, had a significant effect on product content **5**. Also, the lack of fit test was found to be nonsignificant. It could be inferred from the data that a higher temperature is preferable to maximize the product content of **5** in the reaction. This is in line with the previous observation; the higher the temperature, the more the starting material content **4** reacts, decreasing its amount and increasing the final product content **5**. The model adequately explains the variation observed in the data, as the predicted R^2 of 0.9817 is in reasonable agreement with the adjusted R^2 of 0.9849. Almost 98% of the change in the response is explained by the effect of temperature.

The final regression equation in terms of coded factors for the content of **5** was as follows:

$$\text{content of } \mathbf{5}(\%) = +47.55 + 45.05 \times \text{C}$$

Statistical Analysis for Degradation Impurity Content 2. On analysis, the results based on the half-normal plot, Pareto

https://doi.org/10.1021/acsomega.4c01293
ACS Omega 2024, 9, 30327−30349

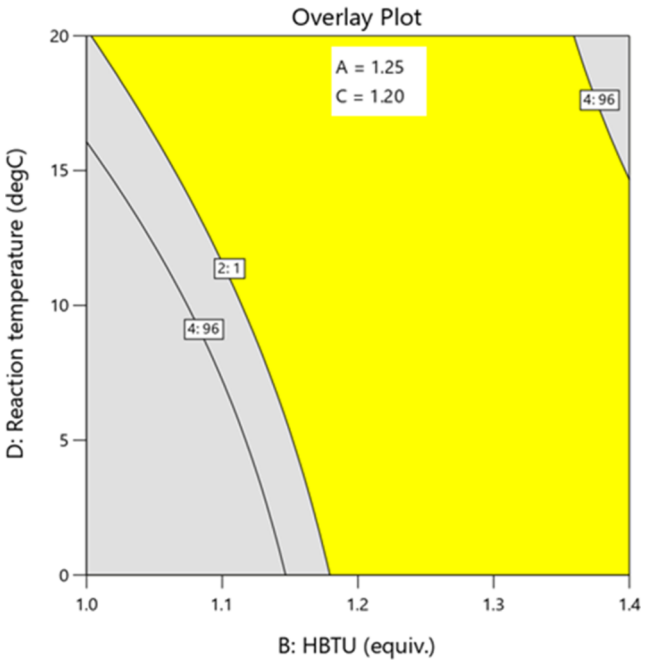

Figure 13. Design space/overlay plot.

Table 11. Acceptable Ranges for the Factors

process parameters	parameter values
boc piperazine equiv	1.25−1.4
HBTU equiv	1.2−1.4
TEA equiv	1.0−1.2
reaction temperature (°C)	5−15

Table 12. Parameters for the DoE Study

factor	parameter	units	type	−1 (low)	+1 (high)
A	methanol	vol	numeric	1	5
B	2 N HCl	vol	numeric	5	12
C	temperature	°C	numeric	25	60

chart (Figure 16), and p-value (<0.05) of the ANOVA statistic (Table 16) showed that reaction temperature has a significant positive effect and methanol vol has a negative effect on the formation of degradation impurity **2**. The 2FI between methanol volume and temperature is also present. From the interaction plot (Figure 17), it can be inferred that when the temperature is higher, the effect of methanol vol on the impurity content is more evident than when the temperature is lower. Higher temperature favors the reaction product, as previously concluded; hence, higher methanol content would help to keep the impurity generation in check. The lack of fit test was not measured due to zero pure error. The predicted R^2 of 0.7949 is in reasonable agreement with the adjusted R^2 of 0.9180.

The final regression equation in terms of coded factors for the content of **2** was as follows:

$$\text{content of } \mathbf{2}(\%) = +2.05 - 1.22 \times \text{A} + 1.42 \times \text{C} - 0.9637 \times \text{AC}$$

Summary for Deprotection Step. For the deprotection step, the reaction temperature was a critical factor among all of the responses selected for this study. The higher temperature was required to intensify the reaction conversion, but at the same time, a higher temperature and lower methanol vol led to the formation of a degradation product **2**. Acid strength was found to be an insignificant factor for all of the responses studied in this reaction step and hence selected at lower vol. Process control was established by taking higher vol of methanol, lower vol of HCl, and higher temperatures to achieve more than 99% reaction conversion and 95% selectivity (Table 17).

The isolation process was optimized to isolate product **5** with more than 99% purity and 90% yield by controlling water volumes and isolation temperatures (Table 18).

Optimization Study of Acylation Step. As reported in the literature, acylation of compound **5** is carried out with compound **6** using DCM as a solvent in the presence of TEA, followed by water treatment to afford compound **1** (Scheme 4) with 83% yield and 99.5% purity. Based on risk assessment, the effect of CPC **6** quantity, TEA quantity, DMF volumes, and CPC addition temperature was studied in the optimization study to maximize the reaction conversion (Table 19). Based on screening experimental data, reaction time was kept constant for 2h. I-Optimal design with two lack of fit points and two replicate points was selected for the study.

Experimental Results and Responses for Statistical Analysis. After the experiments were conducted, reaction conversion (the content of **5**) and formation of required product **1** were measured by HPLC by area normalization. The data demonstrated that the content of **5** (unreacted starting material) varied from 0.01 to 6.66% and that of **1** was from 92.38 to 98.85% (Table 20). Nearly 95% conversion was obtained for most of the runs, and a low starting material was observed. All of the responses were analyzed to find the optimum settings to maximize the reaction conversion and selectivity.

Statistical Analysis for Content of 5. Based on the results, four main effects, one 2FI effect, and two quadratic effects were significant (Table 21). The lack of fit test was found to be nonsignificant. Results obtained based on individual effects plot, interaction effects plot, and ANOVA statistics, the parameters that greatly affect reaction conversion **5** were found to be CPC equiv, CPC addition temperature, TEA equiv, and DMF vol, along with 2FI between CPC equiv and CPC addition

Scheme 3. Synthesis of Intermediate 5

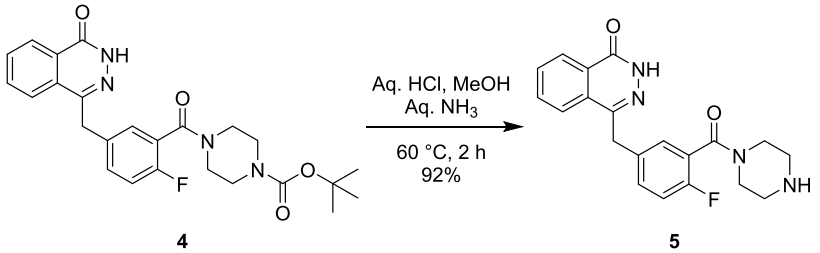

https://doi.org/10.1021/acsomega.4c01293
ACS Omega 2024, 9, 30327−30349

Table 13. Design Layout Along with Responses

run	A: methanol (vol)	B: 2 N HCl (vol)	C: temperature (°C)	4 (%)	5 (%)	2 (%)
1	3	8.5	42.5	54.9	43.1	0.5
2	1	12	60	0.08	92	6
3	5	12	25	93.6	4.31	0.43
4	5	5	60	0.24	93.4	0.99
5	1	5	25	85.44	7.44	1.75
6	1	5	60	0.03	92.59	5.3
7	5	12	60	0.05	96.58	1.59
8	5	5	25	95.77	2.33	0.34
9	1	12	25	94.2	3.9	0.03
10	3	8.5	42.5	62	36.01	0.5

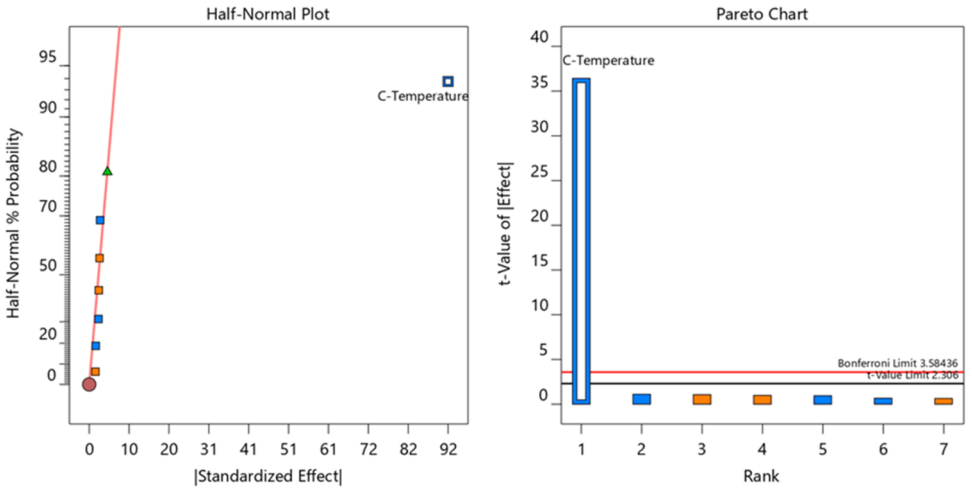

Figure 14. Half-normal plot and Pareto chart for the content of **4**.

Table 14. ANOVA for Content of 4[a]

source	sum of squares	df	mean square	*F*-value	*p*-value	
model	16 984.17	1	16 984.17	410.92	<0.0001	significant
C-temperature	16 984.17	1	16 984.17	410.92	<0.0001	
residual	330.66	8	41.33			
lack of fit	305.45	7	43.64	1.73	0.5279	not significant
pure error	25.21	1	25.21			
cor total	17 314.82	9				

[a]Fit statistics R^2 = 0.9809, adjusted R^2 = 0.9785, and predicted R^2 = 0.9736.

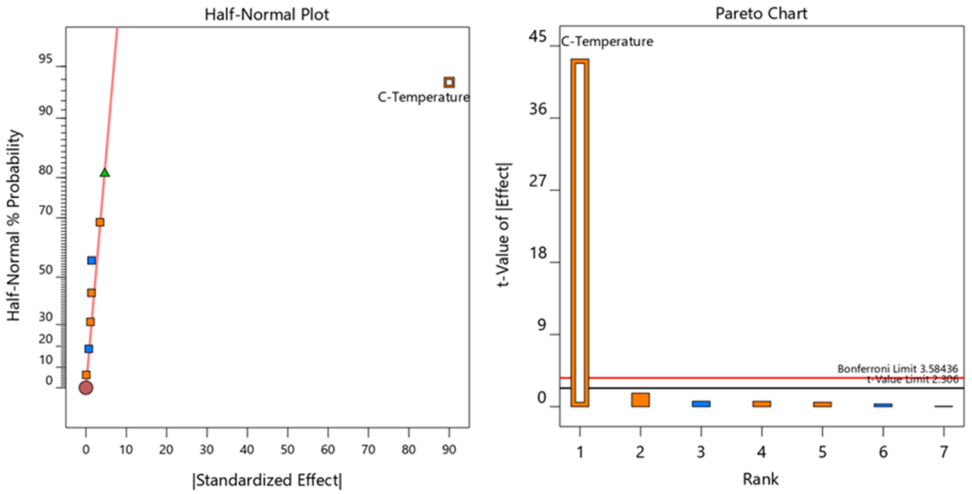

Figure 15. Half-normal plot and Pareto chart for the content of **5**.

https://doi.org/10.1021/acsomega.4c01293
ACS Omega 2024, 9, 30327−30349

Table 15. ANOVA for Content of 5[a]

source	sum of squares	df	mean square	*F*-value	*p*-value	
model	16 236.92	1	16 236.92	589.93	<0.0001	significant
C-temperature	16 236.92	1	16 236.92	589.93	<0.0001	
residual	220.19	8	27.52			
lack of fit	195.05	7	27.86	1.11	0.6261	not significant
pure error	25.13	1	25.13			
cor total	16 457.11	9				

[a]Fit statistics R^2 = 0.9866, adjusted R^2= 0.9849, and predicted R^2= 0.9817.

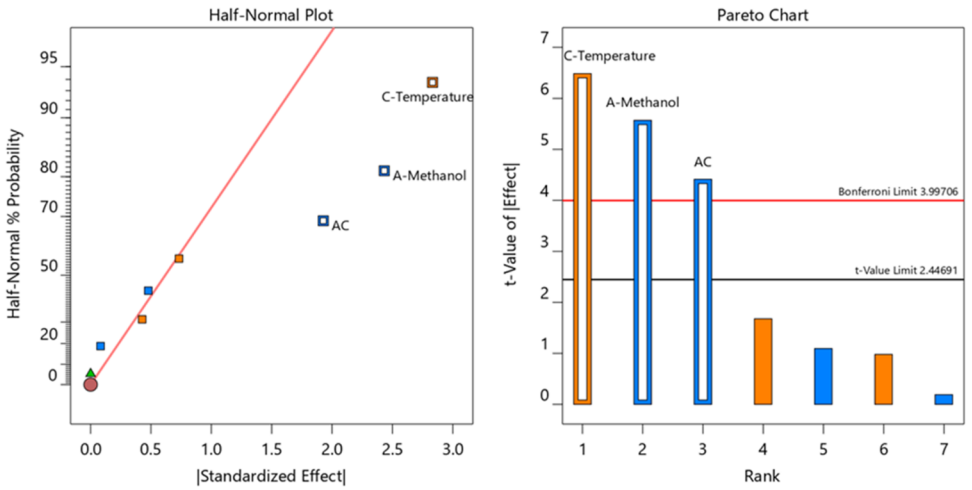

Figure 16. Half-normal plot and Pareto chart for the content of **2**.

Table 16. ANOVA for Content of 2[a]

source	sum of squares	df	mean square	*F*-value	*p*-value	
model	35.31	3	11.77	30.84	0.0012	significant
A-methanol	11.83	1	11.83	31.01	0.0026	
C-temperature	16.05	1	16.05	42.04	0.0013	
AC	7.43	1	7.43	19.47	0.0069	
curvature	3.86	1	3.86	10.12	0.0245	
residual	1.91	5	0.3817			
lack of fit	1.91	4	0.4771			
pure error	0.0000	1	0.0000			
cor total	41.08	9				

[a]Fit statistics R^2 = 0.9487, adjusted R^2 = 0.9180, and predicted R^2 = 0.7949.

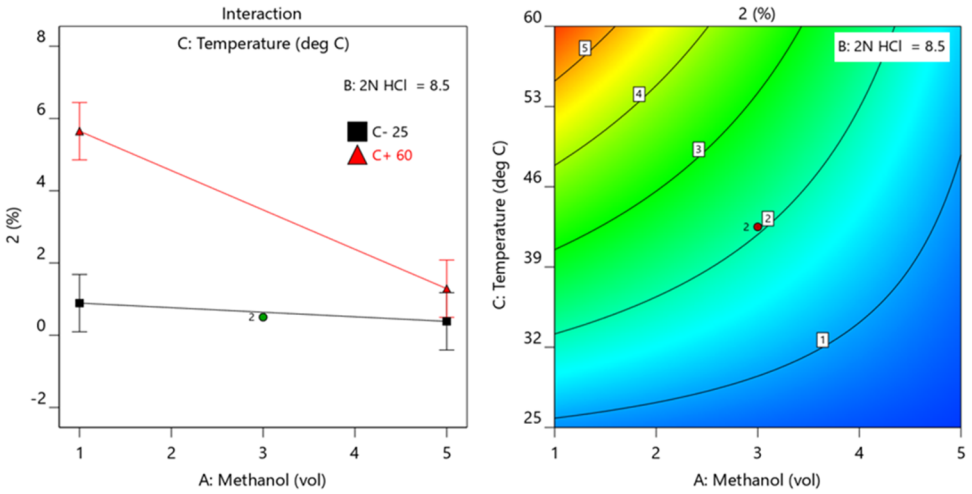

Figure 17. Interaction plot and contour plot for content of **2**.

https://doi.org/10.1021/acsomega.4c01293
ACS Omega 2024, 9, 30327−30349

Table 17. Experimental Results Post DoE

s. no.	methanol (vol)	2 N HCl (vol)	temperature (°C)	4 (%)	5 (%)	2 (%)
1	4	5	65	0.03	96.19	1.89
2	10	5	65	0.05	96.94	1.12
3	5	5	60	0.24	97.22	0.99
4	7	5	55	0.04	97.43	0.88

Table 18. Experimental Results for Isolated Solids

s. no.	methanol (vol)	2 N HCl (vol)	temperature (°C)	4 (%)	5 (%)	2 (%)	Yield (%)
1	5	5	60	0.03	99.31	0.07	91.6
2	5	5	60	0.05	99.32	0.06	89.1

Table 19. Parameters Considered for the DoE Study

factor	parameter	units	type	−1 (low)	+1 (high)
A	CPC	equiv	numeric	1	1.3
B	TEA	equiv	numeric	1	1.5
C	DMF	vol	numeric	5	10
D	CPC addition temperature	°C	numeric	20	50

Scheme 4. Synthesis of Olaparib 1

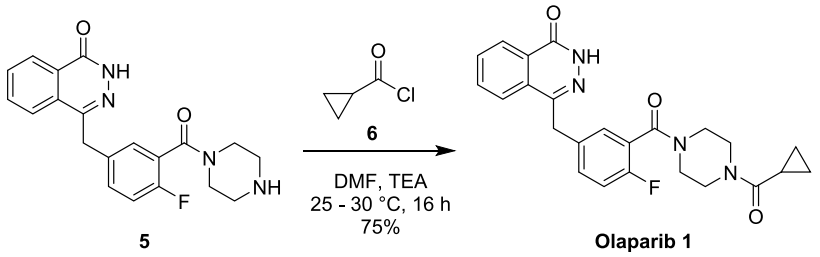

Table 20. Design Layout Along with Responses

run	A: CPC (equiv)	B: TEA (equiv)	C: DMF (vol)	D: CPC addition temperature (°C)	1 (%)	5 (%)
1	1.00	1.17	10.0	50.00	92.38	6.66
2	1.15	1.25	7.5	35.00	98.85	0.02
3	1.00	1.50	6.7	50.00	93.34	5.38
4	1.00	1.25	5.0	20.00	95.64	2.66
5	1.30	1.00	10.0	35.00	98.39	0.01
7	1.10	1.00	5.0	40.00	98.63	0.19
10	1.15	1.00	10.0	20.00	97.99	0.01
11	1.15	1.25	7.5	35.00	98.42	0.01
12	1.30	1.25	10.0	50.00	97.08	0.02
13	1.20	1.50	6.7	20.00	96.09	2.99
14	1.30	1.33	5.0	40.00	97.22	1.76
16	1.30	1.33	10.0	20.00	96.57	2.53
17	1.10	1.00	5.0	40.00	97.03	1.77
18	1.30	1.00	6.7	50.00	96.70	2.42
19	1.30	1.50	7.5	50.00	98.742	0.07
9	1.00	1.00	8.3	20.00	98.61	0.11
15	1.00	1.50	10.0	30.00	98.45	0.01
8	1.30	1.00	5.0	20.00	98.67	0.01
6	1.15	1.50	10.0	50.00	98.02	1.07

temperature (Figures 18 and 19), plus quadratic terms of CPC equiv (A^2) and CPC addition temperature (D^2). Main effects plot of CPC equiv and CPC addition temperature shows that the slope of the curve is large and has a comparatively higher impact on the response with a change in the factor levels. Although significant, TEA equiv and DMF vol have comparatively small slopes. Moderate equiv of CPC and lower addition temperatures are preferable to minimize the content of **5**. Moderate to higher equiv of TEA and higher dilution favored the reaction conversion. The predicted R^2 of 0.8547 is in reasonable agreement with the adjusted R^2 of 0.9155.

The final regression equation in terms of coded factors for the content of **5** is as follows:

https://doi.org/10.1021/acsomega.4c01293
ACS Omega 2024, 9, 30327−30349

Table 21. ANOVA for Content of 5[a]

source	sum of squares	df	mean square	*F*-value	*p*-value	
model	65.16	7	9.31	28.86	<0.0001	significant
A-CPC	33.73	1	33.73	104.58	<0.0001	
B-TEA	5.18	1	5.18	16.06	0.0021	
C-DMF lot-1	2.44	1	2.44	7.56	0.0189	
D-CPC addition temp	8.52	1	8.52	26.42	0.0003	
AD	11.52	1	11.52	35.72	<0.0001	
A^2	10.48	1	10.48	32.49	0.0001	
D^2	3.41	1	3.41	10.56	0.0077	
residual	3.55	11	0.3226			
lack of fit	1.70	9	0.1884	0.2033	0.9640	not significant
pure error	1.85	2	0.9264			
cor total	68.71	18				

[a]Fit statistics R^2= 0.9484, adjusted R^2 = 0.9155, and predicted R^2 = 0.8547.

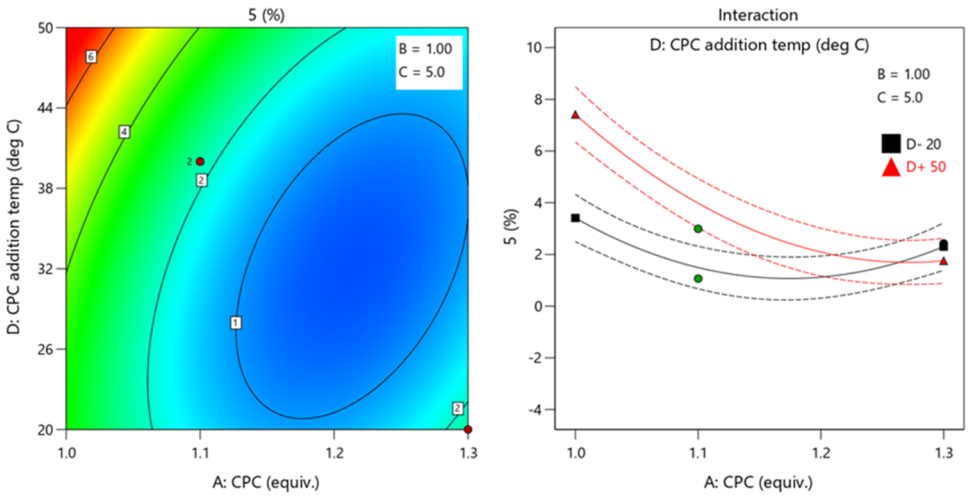

Figure 18. Contour plot and interaction plot for the content of **5**.

Table 22. ANOVA for Content of 1[a]

source	sum of squares	df	mean square	*F*-value	*p*-value	
model	55.25	7	7.89	20.33	<0.0001	significant
A-CPC	24.37	1	24.37	62.78	<0.0001	
B-TEA	1.46	1	1.46	3.76	0.0784	
C-DMF lot-1	1.74	1	1.74	4.48	0.0580	
D-CPC addition temp	3.77	1	3.77	9.71	0.0098	
AD	13.36	1	13.36	34.42	0.0001	
A^2	12.39	1	12.39	31.93	0.0001	
D^2	3.19	1	3.19	8.22	0.0153	
residual	4.27	11	0.3882			
lack of fit	2.39	9	0.2658	0.2832	0.9262	not significant
pure error	1.88	2	0.9387			
cor total	59.52	18				

[a]Fit statistics R^2 = 0.9283, adjusted R^2 = 0.8826, predicted R^2 = 0.7792.

$$\text{content of } \mathbf{5}(\%) = -0.1808 - 1.69 \times A - 0.6858 \times B - 0.4580 \times C + 0.8639 \times D - 1.14 \times AD + 1.74 \times A^2 + 1.02 \times D^2$$

Statistical Analysis for 1. Similar to the previous analysis, based on the results, four main effects, one 2FI effect, and two quadratic effects were significant (Table 22), and the lack of fit test was insignificant. For the results based on individual effects plot, interaction effects plot, and ANOVA statistics, the parameters that greatly affect the formation of **1** were found to be CPC equiv, CPC addition temperature and interaction between CPC equiv and CPC addition temperature (Figures 20 and 21). Moderate equivalents of CPC and lower temperatures are preferred to maximize the content of **1**. Moderate to higher equiv of TEA and higher dilution favored the reaction conversion. The inferences aligned with the outcome from the analysis for the content of **5**. Hence, the model is in sync and adequately explains the variation observed in the data. The

https://doi.org/10.1021/acsomega.4c01293
ACS Omega 2024, 9, 30327−30349

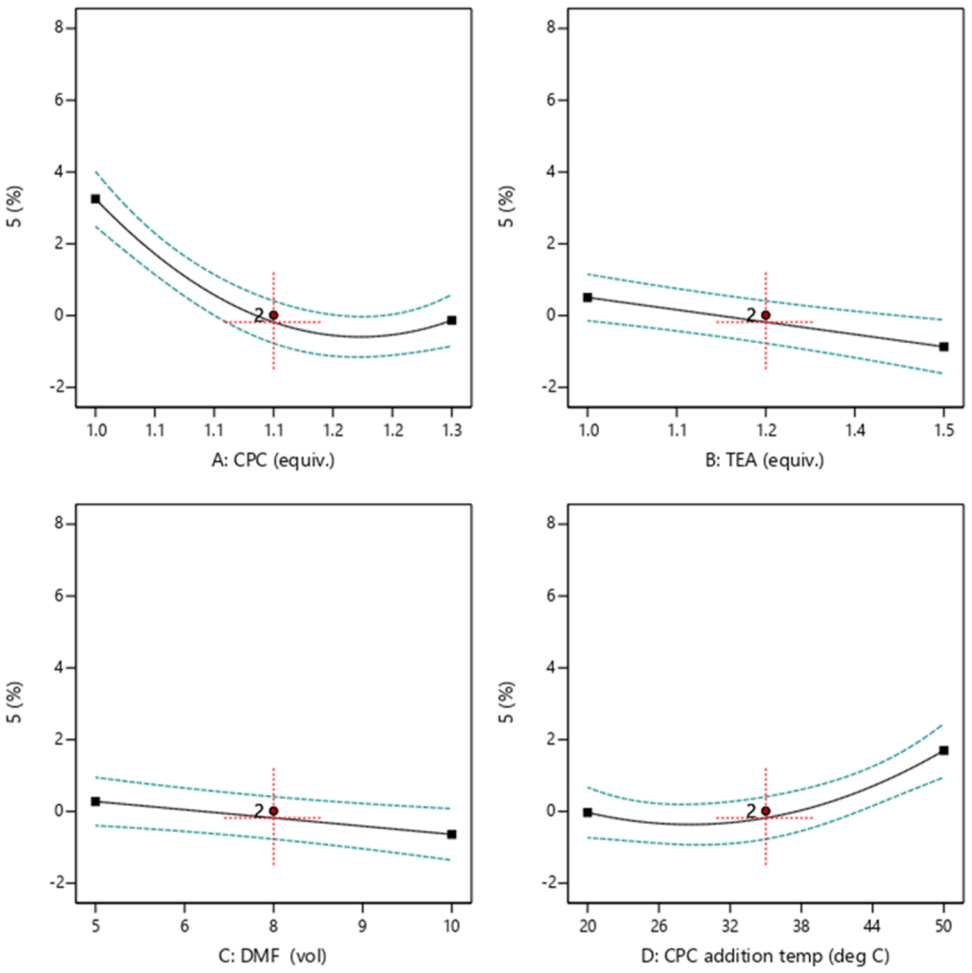

Figure 19. Individual effects plot for the content of **5**.

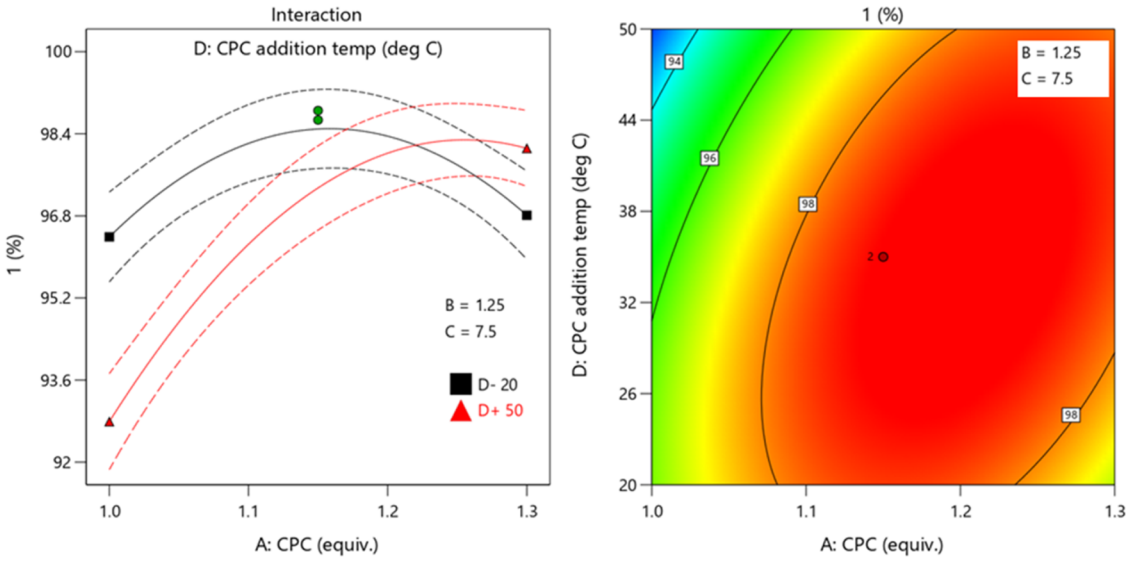

Figure 20. Contour plot and interaction plot for content of **1**.

predicted R^2 of 0.7792 is in reasonable agreement with the adjusted R^2 of 0.8826.

The final regression equation in terms of coded factors for the content of 1 was as follows:

$$\text{content of } \mathbf{1}(\%) = 98.90 + 1.44 \times A + 0.3642 \times B + 0.3866 \times C + -0.5745 \times D + 1.23 \times AD + -1.89 \times A^2 + -0.9828 \times D^2$$

https://doi.org/10.1021/acsomega.4c01293
ACS Omega 2024, 9, 30327−30349

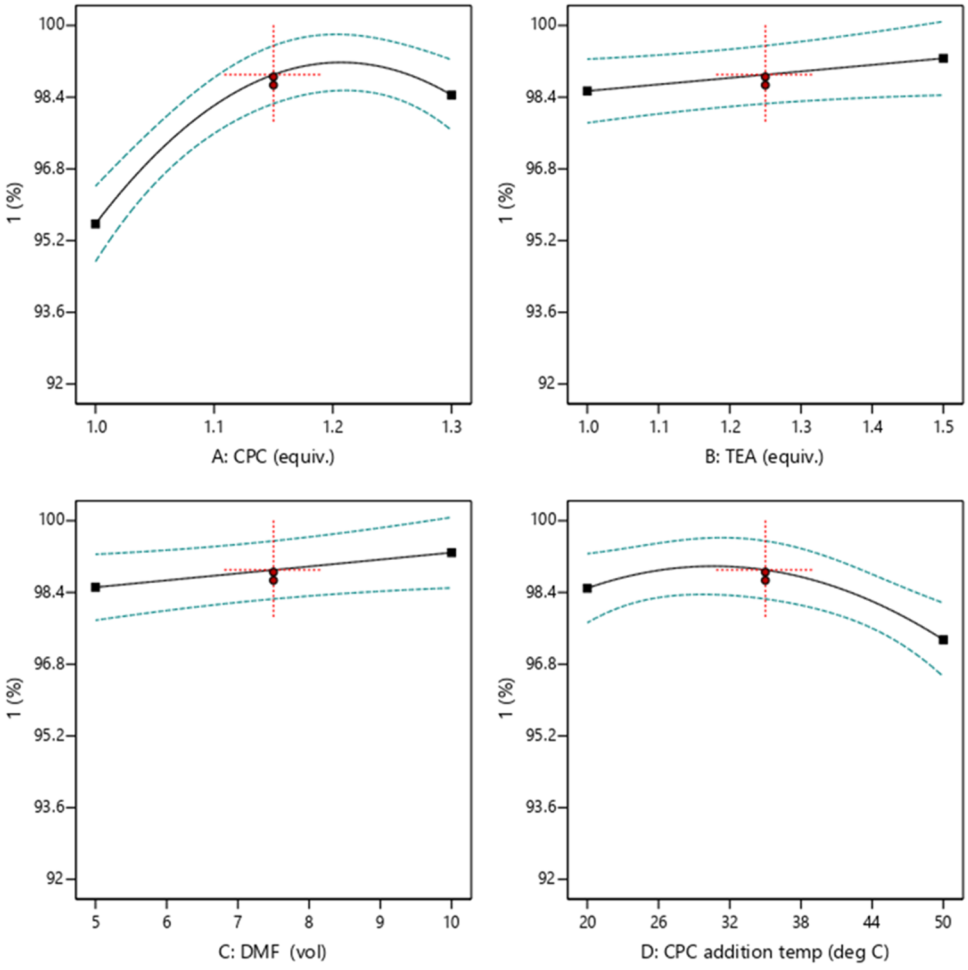

Figure 21. Individual effects plot for the content of **1**.

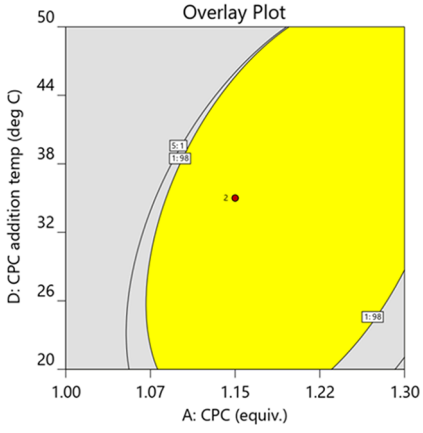

Figure 22. Overlay plot/design space at B = 1.25 and C = 7.5.

Summary for Acylation Step. For the acylation step, CPC equiv and CPC addition temperature were the most critical factors for reaction conversion and selectivity. Moderate equiv of CPC and lower CPC addition temperature was required to maximize the reaction conversion and product formation. Increasing the dilution and using optimum base equiv helps to push the reaction toward maximum conversion. Process control and design space (Figure 22) were established by considering 1.1−1.2 equiv of CPC, 1.15−1.5 equiv of TEA, 7−10 vol of DMF, and 20−35 °C CPC addition temperature to attain more than 99% reaction conversion and 98% selectivity. The isolation process was optimized to isolate product **1** with more than 99% purity.

Green Chemistry Comparatives. Eventually, we compared the greenness of the processes reported by the innovator with the optimized procedure disclosed in this report. It is clearly transpired that the process developed at our end indicated to have lower PMI values, which are manually calculated and cross-verified with a PMI calculator.[15] The details of the PMI evaluation are provided in Figure 23. Our process is greener over the innovator process by ∼170 kg less input per kg of API synthesis by design. Process comparisons are shown in Scheme 5. Further details can be found in the Supporting Information.

CONCLUSIONS

In summary, a quality-by-design methodology using the design of experiments as a tool applied to the development and optimization of Olaparib **1**, enabling a cost-effective, robust process with excellent yields and high purities. Critical process parameters were identified and optimal conditions were established for three chemical conversions using a multivariate experimentation technique. Achieved consistent yields of 95% (**4**), 91% (**5**), and 75% (**1**), respectively, with more than 99% HPLC purity in all three chemical steps leads to overall throughput of 65% with >99.5% HPLC purity for **1** against 38% reported yield. All of the related substances were controlled to below acceptable limits as per ICH guidelines.

https://doi.org/10.1021/acsomega.4c01293
ACS Omega 2024, 9, 30327−30349

(a) PMI Values Based on Innovator Process

- Manual calculation based on the extracted process from literature [11]

  PMI = 259 kg/kg of API

- PMI calculator indicated values

  PMI = 260 kg/kg of API

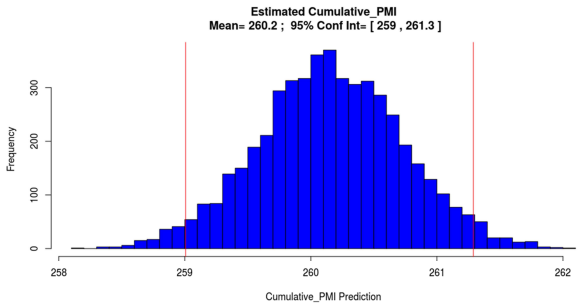

(b) PMI Values Based on Process Disclosed in this Report

- Manual calculation based on process disclosed in this work

  PMI = 88.4 kg/kg of API

- PMI calculator indicated values

  PMI = 88.6 kg/kg of API

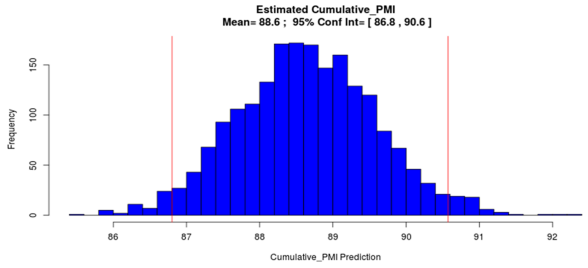

Figure 23. PMI comparatives of the innovator (a) and our process (b).

Scheme 5. Comparison between the Manufacturing Process of DRL and Literature Reported on Olaparib 1

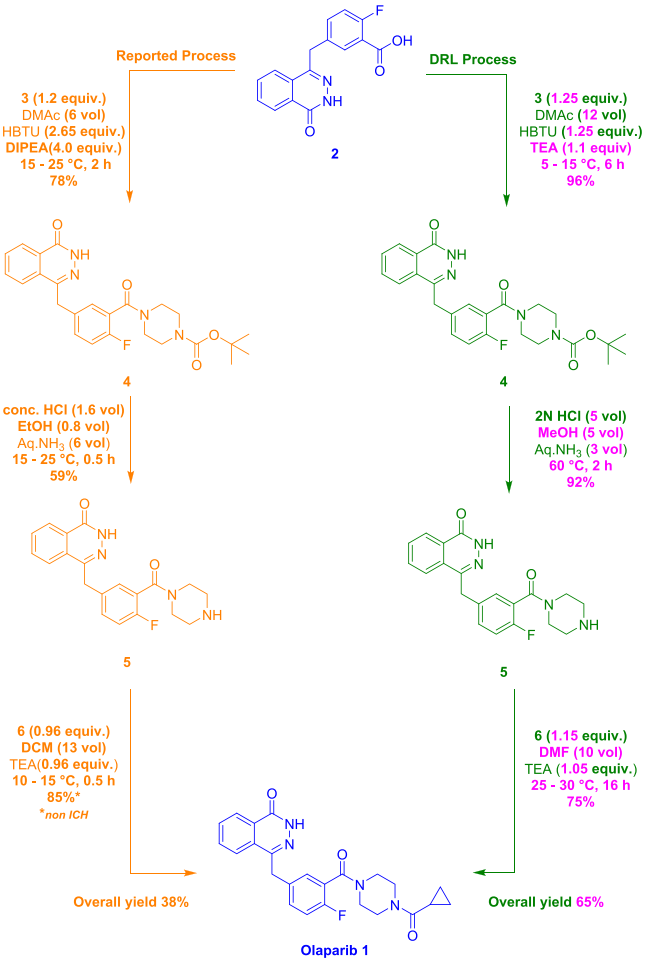

■ ASSOCIATED CONTENT

Supporting Information

The Supporting Information is available free of charge at https://pubs.acs.org/doi/10.1021/acsomega.4c01293.

Experimental procedure, spectral data (^{1}H NMR, ^{13}C NMR, IR, and mass spectral data), and PMI calculations were provided (PDF)

■ AUTHOR INFORMATION

Corresponding Authors

Rakeshwar Bandichhor − *Integrated Product Development Organization (IPDO), Dr. Reddy's Laboratories Ltd., Bachupally, Hyderabad 500090 Telangana, India;* orcid.org/0000-0003-2673-1429; Phone: +91 9000770751; Email: rakeshwarb@drreddys.com; Fax: +91 40 44346285

Arthanareeswari Maruthapillai − *Department of Chemistry, Faculty of Engineering and Technology, SRM Institute of Science and Technology, Kattankulathur 603203 Tamil Nadu, India;* orcid.org/0000-0003-4246-6856; Phone: +91 44 27417832; Email: arthanam@srmist.edu.in

Authors

Amarendhar Manda − *Department of Chemistry, Faculty of Engineering and Technology, SRM Institute of Science and Technology, Kattankulathur 603203 Tamil Nadu, India; Integrated Product Development Organization (IPDO), Dr. Reddy's Laboratories Ltd., Bachupally, Hyderabad 500090 Telangana, India*

Shravan Kumar Komati − *Department of Chemistry, Faculty of Engineering and Technology, SRM Institute of Science and Technology, Kattankulathur 603203 Tamil Nadu, India; Integrated Product Development Organization (IPDO), Dr. Reddy's Laboratories Ltd., Bachupally, Hyderabad 500090 Telangana, India*

Sekhar Munaswamy Nariyam − *Integrated Product Development Organization (IPDO), Dr. Reddy's Laboratories Ltd., Bachupally, Hyderabad 500090 Telangana, India*

Sasikala Cheemalapati Venkata Annapurna − *Integrated Product Development Organization (IPDO), Dr. Reddy's Laboratories Ltd., Bachupally, Hyderabad 500090 Telangana, India*

Gopal Chandru Senadi − *Department of Chemistry, Faculty of Engineering and Technology, SRM Institute of Science and Technology, Kattankulathur 603203 Tamil Nadu, India;* orcid.org/0000-0003-0149-5423

Complete contact information is available at: https://pubs.acs.org/10.1021/acsomega.4c01293

Notes

The authors declare no competing financial interest.

Dr. Reddy's communication number IPDO-IPM-00689

https://doi.org/10.1021/acsomega.4c01293
ACS Omega 2024, 9, 30327−30349

■ ACKNOWLEDGMENTS

The authors are thankful to the management of Dr. Reddy's Laboratories Ltd. We highly appreciate the cooperation from all of the supporting function colleagues for supporting this work. Special thanks to Sridhar Vasam, Dr Kagita Veera Babu, and Veerender Murki for their support in experimentation.

■ ABBREVIATIONS

ANOVA	analysis of variance
API	active pharmaceutical ingredients
BP	boc piperazine
CMA	critical material attribute
CPP	critical process parameter
CPC	cyclopropane carbonyl chloride
CQA	critical quality attribute
DCM	dichloromethane
df	degrees of freedom
DIPEA	*N*,*N*-diisopropylethylamine
DMF	*N*,*N*-dimethylformamide
DoE	design of experiments
DMAc	dimethylacetamide
EDC·HCl	1-ethy-3-(3-(dimethylamino)propyl) carbodiimide hydrochloride
equiv	equivalents
FI	factor interaction
h	hours
HBTU	1-[bis(dimethylamino)methylene]-1*H*-benzotriazolium-3-oxide hexafluorophosphate
HCl	hydrochloric acid
HOBt·H_2O	1-hydroxybenzotriazole monohydrate
HPLC	high-performance liquid chromatography
KMA	key material attribute
KPP	key process parameter
NLT	not less than
NMP	*N*-methyl-2-pyrrolidone
NMT	not more than
QbD	quality by design
R^2	coefficient of determination
RSM	response surface methodology
TEA	triethylamine
vol	volumes

■ REFERENCES

(1) Department of Health and Human Services, U.S. Food and Drug Administration. In *Pharmaceutical Quality for the 21st Century A Risk-Based Approach Progress Report*; Center for Drug Evaluation and Research (CDER): Rockville, MD, 2007.

(2) Department of Health and Human Services, U.S. Food and Drug Administration. In *ICH Q8 Pharmaceutical Development (R2)*; Center for Drug Evaluation and Research (CDER): Rockville, MD, 2009.

(3) Department of Health and Human Services, U.S. Food and Drug Administration. In *ICH Q9 Quality Risk Management*; Center for Drug Evaluation and Research (CDER): Rockville, MD, 2009.

(4) Department of Health and Human Services, U.S. Food and Drug Administration. In *ICH Q10 Pharmaceutical Quality System*; Center for Drug Evaluation and Research (CDER): Rockville, MD, 2009.

(5) Lheureux, S.; Oza, A. M. Olaparib for the treatment of ovarian cancer. *Expert Opin. Orphan Drugs* **2014**, *2*, 497−508, DOI: 10.1517/21678707.2014.899147.

(6) Weissman, S. A.; Anderson, N. G. Design of Experiments (DoE) and Process Optimization. A review of Recent Publications. *Org. Process. Res. Dev.* **2015**, *19*, 1605−1622.

(7) Abe, Y.; Emori, K. Application of a Statistical Approach to Process Development of Futibatinib by Employing Quality-by-Design Principles. Part 1: Identification of Critical Process Parameters for Impurities. *Org. Process. Res. Dev.* **2022**, *26*, 43−55.

(8) Abe, Y.; Emori, K. Application of a Statistical Approach to Process Development of Futibatinib by Employing Quality-by-Design Principles. Part 2: Development of Design Space for Impurities Using the Response Surface Methodology. *Org. Process. Res. Dev.* **2022**, *26*, 56−71.

(9) Abe, Y.; Emori, K. Application of a Statistical Approach to Process Development of Futibatinib by Employing Quality-by-Design Principles. Part 3: Development of Design Space for Control of Particle Size Distribution. *Org. Process. Res. Dev.* **2022**, *26*, 72−81.

(10) Wang, H.; Chen, K.; Lin, B.; Kou, J.; Li, L.; Wu, S.; Liao, S.; Sun, G.; Pu, J.; Yang, H.; Wang, Z. Process Development and Optimization of Linagliptin Aided by the Design of Experiments (DoE). *Org. Process. Res. Dev.* **2022**, *26*, 3254−3264.

(11) Hughes, D. L. Patent Review of Manufacturing Routes to Recently Approved PARP Inhibitors: Olaparib, Rucaparib, and Niraparib. *Org. Process Res. Dev.* **2017**, *21*, 1227−1244, DOI: 10.1021/acs.oprd.7b00235.

(12) Flick, A. C.; Ding, H. X.; Leverett, C. A.; Kyne, R. E.; Liu, K. K. C.; Fink, S. J.; O'Donnell, C. Synthetic approaches to the 2014 new drugs. *J. Bioorg. Med. Chem.* **2016**, *24*, 1937−1980, DOI: 10.1016/j.bmc.2016.03.004. Medicinal Chemistry route summarized in the following review:

(13) (a) Menear, K. A.; Ottridge, A. P.; Londesbrough, D. J.; Hallett, M. R.; Mulholland, K. R.; Pittam, J. D.; Laffan, D. D. P.; Ashworth, I. W.; Jones, M. F.; Cherryman, J. H. Phthalazinone Derivatives US7,692,006 B2, 2010. (b) Menear, K. A.; Ottridge, A. P.; Londesbrough, D. J.; Hallett, M. R.; Mulholland, K. R.; Pittam, J. D.; Laffan, D. D. P.; Ashworth, I. W.; Jones, M. F.; Cherryman, J. H. Phthalazinone Derivatives. US8,247,416 B2, 2012. (c) Menear, K. A.; Ottridge, A. P.; Londesbrough, D. J.; Hallett, M. R.; Mullholland, K. R.; Pittam, J. D.; Laffan, D. D. P.; Ashworth, I. W.; Jones, M. F.; Cherryman, J. H. WO2,008,047,082.2008. (d) Martin, N. M. B.; Smith, G. C. M.; Jackson, S. P.; Loh, V. M., Jr.; Cockcroft, X.-L. F.; Matthews, I. T. W.; Menear, K. A.; Kerrigan, F.; Ashworth, A. WO2,004,080,976.2004.

(14) Stat-Ease ≫ v13 ≫ General Sequence of Analysis ≫ ANOVA Output (statease.com).

(15) PMI Calculator. https://acsgcipr-predictpmi.shinyapps.io/pmi_calculator/.

(16) Montgomery, D. C. *Design and Analysis of Experiments*; John wiley & sons, 2017.

(17) Foschi, M.; Capasso, P.; Maggi, M. A.; Ruggieri, F.; Fioravanti, G. Experimental Design and Response Surface Methodology Applied to Graphene Oxide Reduction for Adsorption of Triazine Herbicides. *ACS Omega* **2021**, *6*, 16943−16954.

(18) Alturkistani, S.; Wang, H.; Gautam, R.; Sarathy, S. M. Importance of Process Variables and Their Optimization for Oxidative Coupling of Methane (OCM). *ACS Omega* **2023**, *8*, 21223−21236.

(19) https://prismtc.co.uk/resources/blogs-and-articles/the-sequential-nature-of-classical-design-of-experiments.

(20) Ramirez, A.; Hallow, D. M.; Fenster, M. D.; Lou, S.; Domagalski, N. R.; Tummala, S.; Srivastava, S.; Hobson, L. A. Development of a control strategy for a final intermediate to enable impurities control. *Org. Process. Res. Dev.* **2016**, *20*, 1781−1791.

https://doi.org/10.1021/acsomega.4c01293
ACS Omega 2024, 9, 30327−30349